

**Examination of induction of innate immune memory
of alveolar macrophages and trained innate immunity
following respiratory exposure to infectious agents**

Examination of induction of innate immune memory of alveolar macrophages and trained innate immunity following respiratory exposure to infectious agents

By: Ramandeep Singh, B.Sc.

Thesis submitted to the School of Graduate Studies in partial fulfillment of the requirements for the Master's of Science degree.

McMaster University

© Copyright, Ramandeep Singh, July 2022

Master’s of Science (2022)

Medical Sciences: Infection and Immunity – McMaster University, Hamilton, Ontario, Canada

Title: Examination of induction of innate immune memory of alveolar macrophages and trained innate immunity following respiratory exposure to infectious agents

Author: Ramandeep Singh (McMaster University)

Supervisor: Dr. Zhou Xing (M.D., Ph.D.)
Professor, Medicine, Clinical Immunology & Allergy

Number of pages: xi, 73

Lay Abstract

The immune system has been classically divided into two major compartments known as the innate and adaptive immune system. For decades, the predominant consensus amongst the field was that only the adaptive immune system can form memory against any pathogens encountered. It has been well established that plants and invertebrates only possess an innate immune system and still show boosted responses and enhanced protection against previously encountered as well as new pathogens. Recently, such capacity for innate immune memory has also been demonstrated in humans and pre-clinical animal models. Innate immune memory provides non-specific, broad-spectrum protection whereas adaptive memory is specific to a singular pathogen. Inducing broad-spectrum protection can be crucial for the future of human medicine. Activation of both adaptive and innate immune arms could prove to be extremely beneficial in vaccination strategies. Through the use of a pre-clinical model, we have found that administering β -glucan, a component of fungal cell wall, directly into the lung significantly alters the phenotype and functionality of lung immune cells, and also provides enhanced protection against a heterologous infection.

Abstract

In the last decade, the potential of β -glucan, a fungal cell wall component, to induce epigenetic and functional modification of innate immune cells, signified as trained innate immunity (TII) has been demonstrated in several pre-clinical and clinical studies. Parenteral administration of β -glucan has resulted in centrally induced TII in the bone marrow/circulating monocytes. Such trained innate immune cells play a critical role in protection against secondary infections. However, there are now indications that inducing local long-lasting immunity at mucosal barrier tissues such as the lung is warranted for protective immunity against respiratory pathogens. Currently, it remains unclear whether respiratory mucosal administration of β -glucan will induce long-lasting resident-memory macrophages and TII and if so, what are the underlying mechanisms of development and maintenance of memory macrophages at respiratory mucosa. To address this, first we have established a murine model where 50 μ g of β -glucan was administered intranasally and kinetics of immune responses in the lung were studied. Profound changes in airway macrophage (AM) pools were observed starting from 3 days post-exposure, which was associated with monocyte recruitment, and this was followed by a series of phenotypic shifts in AMs. The altered AM phenotype profile persisted for up to 8 weeks post-exposure. Importantly, β -glucan-trained AMs demonstrated heightened MHC II expression, enhanced responses to secondary stimulation and improved capacity to perform bacterial phagocytosis. Furthermore, mice with β -glucan-trained AMs displayed higher rates of survival and improved bacterial control, in the lung and periphery, following a lethal *S. pneumoniae* infection. Our findings together indicate that a single intranasal delivery of β -glucan is able to train AMs. Further work into epigenetics, metabolism, and the contribution of AMs in protection is needed.

Acknowledgments

First and foremost, I would like to thank my supervisor Dr. Zhou Xing. Dear Zhou, thank you for everything. Your mentorship, guidance, unwavering support, patience, genuine interest and care in my development and progress through this program. I am extremely grateful for all that you have done for me, the invaluable lessons you have imparted regarding both science and life will stick with me forever. I am incredibly thankful to have had the opportunity to learn and grow in your lab. It has been an amazing experience all thanks to the supportive and collaborative environment that you have fostered.

I would also like to thank my committee members Dr. Yonghong Wan and Dr. Carl Richards for their insight and encouragement. Feedback that I have received from you both has been crucial in my research and growth as a researcher. A big thank you to Dr. Manali Mukherjee for sparing her time and agreeing to participate as the external examiner on my defense committee.

Among lab members, I would like to thank our senior scientist, Dr. Mangalakumari Jeyanathan, for all of her guidance, advice, and scientific support. Mathy, you have been vital in teaching me crucial scientific skills, coming up with ideas for my project, countless meetings to discuss data and progress, and working with me so that I could better myself as a trainee. Thank you for all of the continued help during my time with the lab, I really appreciate it.

A huge thank you, to our lab coordinator Anna Zganiacz. Anna, from training to meaningful conversations, you have been a continued ray of sunshine in the lab. You took Alisha and I under your wings and taught us so many techniques and how to perform them in the correct way. You truly are a pillar of this lab, and I will always admire your commitment to your work and your outlook on life. Thank you so much Anna for everything that you have done for me, I will never forget it.

I would be remiss to not thank Dr. Sam Afkhami for his cherished friendship, unwavering support and countless hours spent teaching me scientific skills. Sam, you have stood by me in every single professional and personal struggle. Anytime I had any problems or stressful situations, without fail you very effectively calmed me, and went on to help me find a solution. I am grateful to have met you, gotten to know the incredibly kind person that you are, and had the opportunity to watch a truly remarkable scientist work. Mike, thank you so much for your incredible help in training, getting my project off the ground, hours of helping me with flow, advice, support, and friendship. Watching you and Sam work alongside each other was an absolute pleasure, your work ethic and passion for science is truly an inspiration to me.

Alisha and Gluke, for your friendships, endless support, encouragement, help with experiments, ideas, and innumerable memories, thank you. Alisha, from beginning in the lab together and getting mouse training to committee meetings, posters and presentations, write-ups, every single experiment, speaker music while doing serial dilutions, isolating bone marrow, and every single up and down, you have always been there with me. I am so thankful to have met you and that I had the opportunity to foster a great friendship, grow, and learn alongside you. Gluke, you are like the younger sister I always wanted, working with you, making mistakes, learning from them, and

laughing uncontrollably is something I will miss. I am also very thankful to Zhou for providing us three the opportunity to attend a conference together, that trip was unforgettable.

To my parents, who left their ancestral homes behind in beautiful Punjab and immigrated to an unfamiliar country so that their kids could have a better quality of life, I do not know how I could possibly begin to thank you. For endless sacrifices, unconditional support, values, work ethic instilled in us, and the immeasurable number of other things that you have done and continue to do, I am forever grateful and thankful. Your dream was to come to this country and to provide us with higher education so that we may better ourselves, and you did it.

A very special thank you to my sisters, Navreet Brar and Dr. Harinder Singh, without you both I would not be here. You both are my inspiration, safe space, and best friends. Indu, you are also my third parent, and I had the honour of watching you work ferociously to defeat all the odds and achieve your professional and personal goals. I am thankful and proud to be a brother to you both, without you I would not be the person I am today.

List of figures

Diagram 1: Conceptual summary of the effects of β -Glucan following intranasal delivery

Figure 1: Respiratory mucosal delivery of an Ad-vectored vaccine generates memory AMs with upregulated MHC II expression.

Figure 2: Inflammatory cellular responses in the airways at 7 days following intranasal delivery of a low dose (LD) or high dose (HD) of β -Glucan.

Figure 3: Significant and persistent alterations in the airway cellular profile and macrophage phenotype at various timepoints post-intranasal delivery of β -Glucan.

Figure 4: Time-dependent upregulation of MHC II expression in airway macrophages following intranasal delivery of β -Glucan.

Figure 5: Significant recruitment and differentiation of circulating monocytes to bona fide AMs following intranasal delivery of β -Glucan

Figure 6: Cytokine production by Ad vaccine- or β -Glucan-trained airway macrophages in response to ex vivo re-stimulation with inflammatory agents (WCL or LPS).

Figure 7: Changes in circulating monocytes following intranasal delivery of β -Glucan.

Figure 8: Assessment of bacterial phagocytosis and killing by β -Glucan-trained airway macrophages.

Figure 9: Differential airway cellular responses to intranasal delivery of β -Glucan and Ad-vectored vaccine.

Figure 10: TII elicited by intranasal delivery of β -Glucan or Ad-vectored vaccine provides enhanced protection against clinical outcomes from heterologous *S. pneumoniae* infection.

Figure 11: TII elicited by intranasal delivery of β -Glucan or Ad-vectored vaccine provides enhanced control of *S. pneumoniae* infection in the lung.

Figure 12: Repeat assessment of intranasal β -Glucan exposure-mediated protection against heterologous bacterial infection.

Figure 13: Differential airway immune responses to *S. pneumoniae* infection following intranasal delivery of β -Glucan and Ad-vectored vaccine.

Supplementary Figure 1: Gating strategy for identification of pulmonary macrophage populations

Supplementary Figure 2: Naïve airways have a small population of SF^{lo} AMs that is differential to populations seen following intranasal delivery of β -Glucan.

List of abbreviations:

Abbreviation	Full Terminology
Ad	Adenovirus
AM	Alveolar macrophage
ANOVA	Analysis of variance
BAL	Bronchoalveolar lavage
BCG	Bacillus Calmette–Guérin
DC	Dendritic cell
ECAR	Extracellular acidification rate
HDM	House dust mite
HSC	Hematopoietic stem cell
HSPC	Hematopoietic stem cell progenitor
IAV	Influenza A Virus
IM	Interstitial macrophage
i.n	Intranasal
i.p	Intraperitoneal
i.t	Intratracheal
i.v	Intravenous
LPS	Lipopolysaccharide
MdM	Monocyte-derived macrophage
MFI	Median fluorescence intensity
MOI	Multiplicity of infection
MMR	Measles Mumps Rubella
Mtb	<i>Mycobacterium tuberculosis</i>
OPV	Oral polio vaccine
PBS	Phosphate saline buffer
PRR	Pattern recognition receptor
RM	Respiratory mucosal
TII	Trained innate immunity
Trans AM	Transitioning alveolar macrophage
WCL	<i>M.tb</i> Whole cell lysate

Table of Contents

<i>Lay Abstract</i>	<i>iv</i>
<i>Abstract</i>	<i>v</i>
<i>Acknowledgments</i>	<i>vi</i>
<i>List of figures</i>	<i>viii</i>
<i>List of abbreviations:</i>	<i>ix</i>
1.0 – Introduction	2
1.1 – Research overview	3
1.2 – Innate immune memory: a new paradigm shift	4
1.3 – Induction of innate immune memory and TII following systemic exposure to live organisms	6
1.4 – Induction of innate immune memory and TII following systemic exposure to inflammatory agonists	8
1.5 – Cellular and molecular mechanisms of TII	11
1.6 – Metabolic and epigenetic mechanisms of TII	12
1.7 – AMs in respiratory host defense	13
1.8 – Role of AMs in host defense against respiratory <i>Streptococcus pneumoniae</i> infection	14
1.9 – Current understanding of innate immune memory of AMs and TII in the lung	15
1.10 – Properties of β-Glucan	17
1.12 – Project significance	21
2.0 – Materials and Methods	22
3.0 – Results	29
3.1 – Respiratory mucosal delivery of adenoviral-vectored vaccine gives rise to memory AMs	30
3.2 – Inflammatory cellular responses in the airways following intranasal delivery of a low dose or high dose of β-Glucan	30
3.3 – Significant and persistent alterations in the airway cellular profile and macrophage phenotype at various timepoints post-intranasal delivery of β-Glucan	32
3.4 – Time-dependent upregulation of MHC II expression in airway macrophages following intranasal delivery of β-Glucan	33
3.5 – Significant recruitment and differentiation of circulating monocytes to bona fide AMs following intranasal delivery of β-Glucan	34
3.6 – Cytokine production by Ad vaccine- or β-Glucan-trained airway macrophages in response to ex vivo re-stimulation with inflammatory agents	35
3.7 – Changes in circulating monocytes following intranasal delivery of β-Glucan	36

3.8 – Assessment of bacterial phagocytosis and killing by β-Glucan-trained airway macrophages	37
3.9 – Differential airway cellular responses to intranasal delivery of β-Glucan and Ad-vectored vaccine	38
3.10 – TII elicited by intranasal delivery of β-Glucan or Ad-vectored vaccine provides enhanced protection against clinical outcomes from heterologous <i>S. pneumoniae</i> infection	40
3.11 – TII elicited by intranasal delivery of β-Glucan or Ad-vectored vaccine provides enhanced control of <i>S. pneumoniae</i> infection in the lung	41
3.12 – Differential airway immune responses to <i>S. pneumoniae</i> infection following intranasal delivery of β-Glucan and Ad-vectored vaccine	42
4.0 – Discussion	44
Future Directions	50
5.0 – References	52
6.0 – Figures	58

1.0 – Introduction

1.1 – Research overview

The central dogma of immunological memory postulates that the adaptive immune system can retain information about an antigen, following primary exposure, and upon secondary exposure will be able to launch a rapid and robust response via memory T and B effector cells. Although the concept of innate immune memory in plants and invertebrates has been previously well established, in recent years there has been a paradigm shift occurring in regard to innate immune memory in vertebrates. Innate immune memory is defined as a reset state of the innate immune system following initial antigen or microbial exposure, this can lead to altered responsiveness to the same or unrelated antigen or microbe. Furthermore, this altered responsiveness can encompass either a state of hyperresponsiveness upon secondary exposure, termed Trained Innate Immunity (TII), or a state of hypo-responsiveness which has been termed as tolerization. Characteristics of TII include a pro-defense signature, increased cytokine responses, metabolic/epigenetic re-wiring, and enhanced protection against heterologous infections.

Live attenuated vaccines such as *Bacillus Calmette–Guérin* (BCG), Measle Mumps Rubella (MMR) and Oral Polio Vaccine (OPV) have been shown to generate non-specific protection in humans. There are many gaps in knowledge regarding the induction of TII when pursued by different routes (systemic vs local mucosal) and with different types of inflammatory/infectious agents (live pathogen vs agonist). Currently, most of the work done in the field with various inflammatory/infectious agents such as BCG, live *C. albicans*, β -Glucan, LPS etc. has been conducted in the context of systemic exposure and shown to induce innate immune memory and TII in circulating monocytes. Limited knowledge exists regarding the effects of local respiratory mucosal (RM) exposure to infectious agents on tissue-resident macrophages

Given that the respiratory tract is prone to exposure to an array of infectious agents, it is important to learn more about the benefits and caveats of innate immune memory and TII in the lung. Alveolar macrophages (AMs) are the major tissue-resident innate immune cells in the airways and the first line of defense against invading pathogens. AMs are of embryonic origin and under homeostatic conditions can proliferate *in situ* without replenishment from blood monocytes. Our lab has shown that respiratory mucosal delivery of an adenovirus (Ad)-vectored vaccine can induce a memory-like phenotype in AMs. Memory AMs exhibit an increased capacity to secrete neutrophil recruiting chemokines, resulting in better protection against *S. pneumoniae* infection compared to AMs from naïve counterparts. Since β -Glucan (a polysaccharide abundant in the fungal cell wall) has been widely used in systemic models of TII, this project has focused on evaluating whether local mucosal delivery of β -Glucan induces memory AMs, and if so, whether it invokes TII in the lung. This project serves to fill important knowledge gaps in this young field that could result in changes in vaccination strategies and increase knowledge about TII in respiratory mucosal tissue.

1.2 – Innate immune memory: a new paradigm shift

Traditionally, the two divisions of the immune system, innate and adaptive, are known to have distinct characteristics. Established under that dichotomy is the notion that the innate immune system launches a rapid but non-specific response whereas the adaptive immune system generates a slower but specific response, with the outcome of long-lasting immunological memory¹. Growing evidence has shown that the innate immune system can assume certain characteristics of the adaptive immune system. Pattern Recognition Receptors (PRRs) of the innate immune system maintain some specificity in their recognition of microorganisms² and growing evidence suggests

that the innate immune system may alter its responses after a primary insult³. Furthermore, plants and invertebrates, which lack an adaptive immune system, and even mammals have shown protection against infection by secondary related/unrelated pathogens^{4,5}. This emerging understanding of the innate immune system has been termed innate immune memory which encompasses either the hyper-responsiveness state known as trained innate immunity, or the hypo-responsive state known as innate immune tolerance. Thus, it is our view that innate immune memory and TII are not to be interchangeably used⁶. In contrast to adaptive memory, memory formation in the innate immune system involves an entirely different set of cells, such as myeloid cells, NK cells and innate lymphoid cells. Pattern recognition receptors also play an important role in the induction of innate immune memory, allowing for enhanced microbe detection and contribute to enhanced cytokine production⁷. An augmented response upon secondary stimulation is an essential component of TII and the mechanisms by which this improved non-specific responsiveness is maintained, are signals affecting transcription factors and epigenetic reprogramming⁷. This altered state of responsiveness has been documented to be maintained for weeks to months rather than years, which is a hallmark of the adaptive immune system⁷. As more work is being conducted in this rather new and evolving field, there remains much to be discovered about the array of mechanisms by which innate immune memory and TII may be generated and maintained. Further knowledge of the mechanisms underlying this phenomenon could be used to develop new therapeutic and vaccination strategies.

1.3 – Induction of innate immune memory and TII following systemic exposure to live organisms

Live attenuated vaccines such as BCG and MMR have been shown to portray non-specific protective effects against acute lower respiratory tract infection caused by RSV in humans^{8,9}. BCG is a live-attenuated form of *Mycobacterium bovis* and to date is the only clinically approved vaccine against TB. This vaccine is administered through the parenteral route shortly after birth in most countries and while effective against childhood disseminated tuberculosis, it remains ineffective against pulmonary tuberculosis in adults¹⁰. Developed over 90 years ago, non-specific protective effects of this vaccine in reducing childhood mortality were observed as early as the 1930s¹¹. BCG vaccinated individuals in Guinea-Bissau were associated with lower incidence of hospitalization from acute lower respiratory tract infections due to RSV⁹. Furthermore, BCG vaccination altered bone marrow hematopoietic stem cell progenitors (HSCPs), particularly the myeloid progenitors, which gave rise to trained monocytes in the peripheral blood of human participants¹². Monocytes from periphery also displayed key characteristics of TII; enhanced cytokine recall response and certain histone modifications. Notably, the trained phenotype in peripheral monocytes persisted 90 days following vaccination, pointing to the potential for long lasting training¹². Interestingly, BCG is also a commonly used therapy for patients with bladder cancer and the mechanism underlying its efficacy has been postulated to be due to trained innate immunity¹³.

Since the emergence of the COVID-19 pandemic, BCG and its potential protective effects against the virus has been a topic of great interest. There have been more than 20 trials conducted/being conducted to assess the protective efficacy of BCG against COVID-19¹⁴. The results are varying

and seem to be mixed without a clear consensus. A double-blind randomized trial conducted in Greece, found that BCG revaccination in the elderly (≥ 65) decreased the incidence of SARS-CoV-2 infection. Furthermore, in individuals who were infected, BCG revaccination also reduced the rate of active SARS-CoV-2 respiratory infection¹⁵. Overall, the authors attributed enhanced protection to increased cytokine levels seen in monocytes isolated from BCG revaccinated participants. Overall, BCG is a versatile vaccine/training agent that has many possible applications in health and medicine.

Work in animal models has also shown that systemic administration of this vaccine is capable of educating hematopoietic stem cells (HSCs) and activating myelopoiesis. This generated trained circulating monocytes, which upon infection with *Mycobacterium tuberculosis* (*Mtb*), differentiated into monocyte-derived macrophages (M_{DM}s) in the lung and providing robust protection¹⁶. Trained monocytes were shown to exhibit transcriptional and epigenetic alterations when compared to monocytes of naïve mice¹⁶. BCG vaccination in mice also resulted in enhanced protection against secondary infection with influenza A virus (IAV)¹⁷. Furthermore, BCG has been shown to train NK cells isolated from human volunteer, resulting in an increased production of pro-inflammatory cytokines when stimulated with *Mtb* and unrelated pathogens. In the same study, BCG vaccination increased rates of survival in SCID mice after infection with a lethal dose of *Candida* (*C.*) *albicans*; increased survival was related to trained NK cells¹⁸. Besides monocytes and NK cells, a recent study has shown that BCG vaccination can induce long-term functional re-programming of human neutrophils¹⁹. Discovery of non-specific protective effects from vaccines and further knowledge of BCG's ability to train innate immune cells can have major implications

in understanding current and developing future vaccination strategies with innate immune memory and TII taken into consideration.

Besides BCG, systemic exposure to live pathogens has also been shown to induce TII. In a murine model, a group set out to assess the effects of systemic exposure to a low dose of live *C. albicans*²⁰. A week later, the mice were challenged with a lethal dose of *C. albicans*. Priming with a low dose of the live organism resulted in increased survival and protection against lethal challenge²⁰. *Ex-vivo* work documented enhanced pro-inflammatory cytokine production by trained circulating monocytes upon secondary stimulation. Trained circulating monocytes were also attributed to the prolonged survival of mice, lacking T and B cells, following lethal challenge with *C. albicans*²⁰. Enhanced innate immune protection was found to be accompanied with noteworthy chromatin marker reprogramming in isolated monocytes²⁰. Furthermore, another group utilized systemic administration of live *Mtb* to examine the effects on HSCs. *Mtb*, through the type 1 IFN axis, reprogrammed HSCs to suppress myelopoiesis and impair the generation of trained cells able to provide protection against a secondary infection²¹. Taken together, it is clear that not all live infections/infectious agents are equal in their capacity to invoke TII. In conclusion, systemic exposure to live organisms may invoke innate immune memory and TII associated with an array of different cell types.

1.4 – Induction of innate immune memory and TII following systemic exposure to inflammatory agonists

Systemic exposure to purified microbial components or inflammatory agonists has also been shown to induce similar training effects as systemic exposure to live organisms. β -Glucan is a

widely used microbial component in the field of TII. It is a polysaccharide component of fungal cell walls and has been used in traditional Chinese medicine for centuries²². β -Glucan is an important PAMP following infection with various fungi. The immunomodulatory capabilities of this molecule render it a powerful inflammatory agent. Various membrane-bound immunological receptors, such as dectin-1, scavenger receptors and complement receptor 3, can recognize and bind to β -Glucan, triggering downstream immunological pathways²².

One group purified β -Glucan from *C. albicans* and incubated it with purified monocytes, isolated from healthy human volunteers. β -Glucan-pre-exposed monocytes displayed increased capacities to secrete pro-inflammatory cytokines when stimulated with inflammatory agents such as LPS, live *C. albicans* and *M.tb*²⁰. Interestingly, monocytes pre-exposed to purified β -Glucans or low dose of *C. albicans* responded similarly to secondary stimulation. Training of these monocytes by exposure to β -Glucan was found to be dependent on the dectin-1 receptor as well as the noncanonical Raf-1 pathway²⁰. The same study also showed that the training of monocytes was accompanied with epigenetic changes and notably trimethylation of the histone H3K4²⁰. A recent study showed that a single intraperitoneal administration of 1mg of β -Glucan to C57/BL6 mice resulted in an expansion of myeloid progenitor cells²³. This was accompanied with an increased secretion of IL-1 β and GM-CSF, as well as changes to the glycolytic metabolism in the same cells. The same group also found that β -Glucan-exposed mice displayed enhanced responses upon secondary challenge with LPS²³. Furthermore, in this study, β -Glucan-exposed mice were more resistant to chemotherapy induced myelosuppression, suggesting that modifications to myeloid progenitors is an essential component for systemically-induced TII²³. Another study similarly used β -Glucan to stimulate PBMCs isolated from human volunteer blood and focused on examining

metabolic changes. The researchers noted a robust upregulation of genes involved in glycolysis. This shift in metabolism from oxidative phosphorylation to aerobic glycolysis in monocytes was attributed to the dectin-1-Akt-mTOR-HIF-1 α pathway²⁴. Furthermore, systemic exposure to β -Glucan can provide enhanced protection in mice challenged with *Leishmania braziliensis* or *Mtb*^{25,26}. β -Glucan is also known to train other innate cells such as NK cells, neutrophils and microglia^{27,28,29}. Overall, it is clear that systemic/ex vivo/in vitro exposure to β -Glucan can result in the training of various innate immune cells. However, a significant knowledge gap remains regarding the effects of exposure to this microbial component in local tissue sites.

Other than β -Glucan, LPS is also a purified microbial component that is capable of inducing TII as well as tolerization. A recent study found that a single systemic exposure to LPS can lead to generation of trained microglia in the brain³⁰. However, repeated exposure to LPS led to tolerization of microglia, suggesting that dose and/or numerous exposure events may alter the outcome of training³⁰. In a separate study, administration of LPS led to the generation of tolerized monocytes showed that subsequent ex vivo exposure to β -Glucan led to partial reversal of the LPS-induced tolerization³¹. Furthermore, ex vivo exposure to β -Glucan recovered the capacity of tolerized monocytes to secrete pro-inflammatory cytokines and was accompanied with a reversal of tolerizing epigenetic changes induced by LPS³¹. Based on current knowledge, between LPS and β -Glucan, it seems that β -Glucan is the better candidate for inducing TII. It appears that systemic exposure not only induces TII in circulating cells but can also induce TII in tissue-resident cells as documented in microglia following systemic exposure to either LPS or β -Glucan^{29,30}. These observations open a new avenue of research to investigate whether local mucosal exposure to such

defined microbial component can induce innate immune memory of tissue-resident macrophages at mucosal sites.

1.5 – Cellular and molecular mechanisms of TII

Much work has been done in the field of TII to ascertain the mechanisms behind the phenomena of heterologous enhanced protection. The diversity of training agents used have shown that there are many different underlying mechanisms responsible for the generation and maintenance of TII. Work done by our lab, in a local respiratory exposure model, found that respiratory mucosal delivery of a replication-deficient Ad-vectored vaccine led to the formation of autonomous memory AMs³². Training occurred independent of monocytic contribution and required direct cell to cell contact with CD8⁺ T cells and T cell-secreted IFN γ ³². In many of the systemic exposure models, the mechanism behind the formation of trained innate immunity relies heavily on progenitor cells from the bone marrow compartment^{16,33}. HSPCs, following administration of the systemic agent, often undergo expansion and phenotypic shift generating a myeloid bias and production of trained myeloid cells^{16,33}. Changes to HSPCs rely on molecular mechanisms of important cytokines such as the IL-1 family, IL-32, IL-37 and IFN γ . Such mechanisms have been established through systemic models using both live infectious agents, such as BCG and *C. albicans*, as well as microbial components such as β -Glucan^{16,33,34,35,36}. TLRs and PRRs also have a very important role to play, inflammatory agents induce TII by interacting with these molecules. For example, dectin-1 interacts with β -Glucan and NOD2 plays a vital role in the BCG training model^{34,37}. TLRs help to recognize the agent and trigger downstream inflammatory, metabolic and epigenetic pathways, and as a result, the expression of these immunomodulatory molecules is upregulated in cells being trained^{34,37}. In conclusion, complex cell to cell interactions, certain key

cytokines and molecules such as TLRs and PRRs, involved in signaling pathways, all play a crucial role in the generation of TII.

1.6 – Metabolic and epigenetic mechanisms of TII

A set of key mechanisms for inducing TII include metabolic and epigenetic modifications to trained innate immune cells. Interactions between β -Glucan and its receptor dectin-1 significantly altered the metabolic and epigenetic profile of exposed cells, similar changes have also been marked in systemic BCG, LPS and local Ad-exposure models^{24,32,38-41}. Interactions between inflammatory agents and their receptors trigger an array of responses including a shift in metabolism towards glycolysis, mediated through the mTOR-HIF1 α pathway²⁴. Trained cells exhibit high rates of glucose consumption, enhanced lactate production and an increase in the NAD⁺/NADH ratio^{24,32}. These cells exhibit a strong shift from oxidative phosphorylation as the dominant metabolic pathway to dependency on glycolysis^{40,41}. Inhibition of mTOR, Akt or HIF1 α resulted in a loss of the training phenomena signifying the importance of this metabolic shift to induce TII²⁴. In conclusion, the metabolic shift of favoring glycolysis over oxidative phosphorylation is a crucial indicator of trained innate cells.

The second key mechanism required are epigenetic modifications that occur in trained cells. During the primary stimulus of an inflammatory agent, specific modifications occur on histones of genes associated with TII, namely trimethylation of H3K4me3 and acetylation of H3K27Ac^{6,12,40}. Epigenetic modifications persist in trained cells long after the inflammatory agent has been cleared and allow for enhanced pro-defense responses⁴²⁻⁴⁴. A shift in metabolism and epigenetic modifications are both of crucial importance in the induction of TII.

1.7 – AMs in respiratory host defense

Respiratory mucosal tissue is constantly exposed to various infectious agents, dust, pollutants and allergens⁴⁵. This site is very vulnerable to infection however, the lung is well equipped with immune cells that are well-equipped to fight invading pathogens. One of the main effector cells in the airways are alveolar macrophages (AMs). These cells are unique because they are yolk-sac or fetal-liver derived, persist in the lung for a prolonged period of time and are capable of proliferating *in situ* under homeostatic conditions^{46,47}. Longevity of these cells has always been a matter of interest and studies have shown that the AM phenotype depends strongly on the lung microenvironment. An adoptive transfer study, under homeostatic conditions, has shown that upon transfer into the alveolar niche, peritoneal macrophages were able to change their transcriptomic profile to be like that of AMs⁴⁸. Of note, acute lung injury models have shown that monocytes enter the niche and differentiate into MDMs which have differential gene expression when compared to bona fide AMs. In long-term lung injury models, it was found that the MDMs persisted in the lung up to 10 months after resolution of the initial infection, and by this time their transcriptional and immunophenotypic profile was identical to that of tissue-resident macrophages⁴⁸. AMs play a vital role in the lung and airways by phagocytosing any particulate matter, secreting important enzymes and cytokines, and they are the first site of contact for any inhaled pathogens. They are key in initiation and maintenance of immune responses in the lung and have an array of mechanisms for doing so⁴⁹. AMs are capable of secreting oxygen metabolites and antimicrobial peptides such as lysozyme are crucial in killing phagocytosed pathogens⁵⁰. Surface receptors, such as TLRs, and scavenge receptors, such as MARCO, allow AMs to recognize antigens and stimulate inflammatory pathways, allowing for upregulation of proinflammatory genes⁴⁶. After phagocytosis, AMs can perform intracellular killing via the low

pH secondary lysosomes. Through the mitochondria, AMs are also able to generate potent ROS species⁵¹. AMs are key in launching the host defense against invading pathogens such as *Streptococcus (S.) pneumoniae* whose engulfment by AMs has been described as the rate-limiting step in infection⁵¹. In conclusion, due to their prolonged life, vital mechanisms in host defense and ability to phenotype-switch in response to the lung microenvironment, AMs are a highly relevant target for the investigation of innate immune memory and TIL.

1.8 – Role of AMs in host defense against respiratory *Streptococcus pneumoniae* infection

Despite being a common member of the respiratory microbiota, *S. pneumoniae* can become a serious pathogen if a virulent strain is present or when co-present with other microbes⁵². The most prevalent cause of death by infection in developed countries is severe community-acquired pneumonia and *S. pneumoniae* is the most common cause of lower respiratory tract infection⁵³. A prerequisite for development of disease is colonization of the nasopharynx by *S. pneumoniae* by adhering to mucosal cells of the upper respiratory tract⁵⁴. The pneumococcal capsular antigen is vital in colonization, invasion, and dissemination of bacteria from the respiratory tract. Mucous secretions by the capsular antigen prevent bacterial clearance and aid with transport of pneumococci to the epithelial surface⁵³. Some of the vital initial receptors involved in recognizing and responding to *S. pneumoniae* include but are not limited to: C-reactive protein, a PRR, which binds to phosphorylcholine in the cell wall of pneumococci and then activates the classical complement pathway⁵⁵; MARCO is a class A scavenger receptor expressed on AMs and in vitro has been shown to bind and uptake *S. pneumoniae*⁵⁶; TLR9 is vital in detecting bacterial DNA and TLR9^{-/-} mice were shown to be highly susceptible to lethal infection from *S. pneumoniae*. TLR9

is key for AMs phagocytosis and killing of pneumococci⁵⁷. Furthermore, AMs can secrete chemokines, cytokines and anti-microbial peptides which contribute to innate immunity against pneumococci⁵⁸.

AMs are the first line of host defense against *S. pneumoniae*, they phagocytose and are capable of killing low numbers of pneumococci^{59,60}. When AMs defense is overwhelmed, they may secrete chemokines to recruit neutrophils to the site of infection. Galectin-3 is a soluble adhesion molecule that has been shown to be a major contributor to the neutrophil recruitment signal in pneumococcal pneumonia and to strengthen neutrophil phagocytosis of pneumococci^{53,61}. Phagocytosis by myeloid cells and opsonization via the classical complement pathway are crucial in clearance of pneumococci from circulation^{62,63}. Host defense against *S. pneumoniae* is crucially dependent on the innate mechanisms of complement, AMs, neutrophils, and adaptive immune cells such as T Cells. AMs are involved in the first contact with *S. pneumoniae* and make up a crucial aspect of the innate immune defense against this bacterium. Therefore, *S. pneumoniae* will serve as an ideal infectious challenge to evaluate TII associated with memory AMs.

1.9 – Current understanding of innate immune memory of AMs and TII in the lung

Current knowledge of innate immune memory and TII in mucosal tissues is limited. The question of if long-lived mucosal tissue-resident macrophages are capable of innate immune memory still remains to be answered^{6,32}. Respiratory mucosal tissue is often subject to exposure to a variety of pathogens including but not limited to *S. pneumoniae*, influenza and adenoviruses. Tissue-resident AMs are the first line of defense against any invading pathogen in the respiratory mucosa and as previously mentioned, they have a slow turnover rate, are of embryonic origin and in a steady state

will self-proliferate^{45,64,65}. Under conditions of inflammation, AMs can be replenished with contributions from blood monocytes^{66,67} or may be maintained independently of blood monocytes⁶⁸.

Our lab has studied the effects of acute respiratory viral infection on innate immune memory in mucosal tissue⁴⁰. Respiratory mucosal infection with a wild type Ad or recombinant Ad-vectored vaccine delivered via the intranasal route resulted in AMs expressing high levels of MHC II and invoked noteworthy differences in their transcriptional profiles when compared to naïve AMs. MHC II^{hi} AMs showed upregulation in most crucial host defense genes, including those involved in antigen presentation, chemotaxis, and defense responses. Ad-exposed AMs also exhibited augmented glycolytic metabolism³². AMs with this phenotype persisted up to 16 weeks post-exposure, indicating the presence of an enduring memory phenotype in these AMs. Memory AMs were self-sustained without contribution from circulating monocytes. Other significant findings from this study were that the direct cell to cell contact of AMs with CD8 T cells and CD8 T cell-derived IFN- γ were critical for the formation of memory AMs. Our study also examined TII associated with viral-induced memory AMs against heterologous bacterial infection in the lung. Ad-induced memory AMs significantly enhanced protection against *S. pneumoniae* in an *in vivo* infection model³².

One group developed a model of local, latent respiratory infection with a gammaherpesvirus (murid herpesvirus 4 – MuV4), followed by exposure to house dust mite (HDM) to induce allergic-asthma⁶⁹. In this local-exposure model, sparse in the field of TII, they found that intranasal inoculation of MuV4 led to an acute depletion of all tissue-resident AMs⁶⁹. The empty niche was

then repopulated by cells of monocytic origin, and these MDMs quickly adopted the phenotype of tissue-resident AMs. 1-month post-infection all AMs in the niche were of monocytic origin and displayed the capacity to dampen dendritic cell (DC) induced T_H2 responses to HDM. These trained AMs, protective against development of allergic asthma, displayed long lasting and enhanced expression of MHC II and Sca-1 receptors⁶⁹. Reinforcing the idea that different markers and functional outcomes are associated with trained innate immunity which seems to be very context (route and agent) dependent. Since much of existing knowledge regarding TII pertains to the peripheral system following systemic exposure to infection/inflammatory agents, studies of such nature are vital in contributing to the current paradigm of innate immune memory and TII following respiratory mucosal exposure to infectious/inflammatory agents.

1.10 – Properties of β -Glucan

β -Glucan are naturally occurring glucose polymers abundant in the fungal cell wall and also present in plants and bacteria⁷⁰. For centuries, β -Glucan fibers have been used in traditional Chinese medicine with known healing properties⁷⁰. In modern medicine, much investigation has been done in respect to these β -Glucan molecules. These molecules share a common structure regardless of the source, which is the backbone of $\beta(1,3)$ -linked β -D-glucopyranosyl units. Fungal β -Glucans are specifically characterized by $\beta(1,6)$ -linked branches coming off the $\beta(1,3)$ backbone^{70,71}. It has been observed by many that the structure of a specific β -Glucan can significantly alter its immunomodulation/inflammatory properties however, the mechanism behind this remains unknown at the time of writing^{70,71}. The documented half-life of β -Glucan in a study where rats received an intravenous injection was 3.8 hours⁷². At this point, the half-life of β -Glucan in the context of TII remains undocumented. A study evaluating the effects of systemic

β -Glucan exposure on clinical signs of illness in a variety of pre-clinical animal models, found that consistent daily intraperitoneal (i.p) injections of 250mg/kg of β -Glucan did not result in body weight loss, body temperature dysregulation or deterioration of other main determinants of health⁷³. The β -Glucan utilized in this project was obtained from InvivoGen and isolated from *Trametes versicolor*. This β -Glucan has a mass of 100kDa is made up of multiple chains of β -Glucans linked to a polypeptide region.

Immunomodulatory and inflammatory properties of β -Glucan have been well documented in the field. In fact, β -Glucan has been investigated in many clinical trials to understand more about the therapeutic potential in medicine. One clinical trial assessing the impacts of 30 days of oral β -Glucan administration on the innate immune system in children with chronic respiratory problems showed that short term oral exposure significantly improved mucosal immunity⁷⁴. A double-blind randomized trial found that consumption of β -Glucan significantly reduced the incidence of respiratory infections and the presence of common cold symptoms⁷⁵. β -Glucan has also been extensively investigated in preclinical and clinical cancer models and found to be a strong therapeutic when coupled with monoclonal antibodies, as an adjuvant in a cancer vaccine, and as an immunostimulatory molecule⁷⁶⁻⁷⁹. Usage of β -Glucan is revolutionizing the landscape of modern health and it is of great importance to explore its potential in all different types of human disease models.

1.11 – Rationale, hypothesis, and specific aims

Rationale: There remain many knowledge gaps in the field of innate immune memory, especially regarding TII in local mucosal tissues⁶. Currently, most of the work in the field of innate immune

memory and TII has been conducted in the context of systemic exposure to various live agents and microbial components. It has been well-established that parenteral administration of training agents such as BCG, β -Glucan, LPS and others can result in the training of various innate cell types and provide enhanced protection against an array of heterologous secondary infections^{16,17,20,26,30,31,79,80,81}. Persistent changes to progenitor cell profiles in the bone marrow give rise to trained innate cells such as monocytes, neutrophils and NK cells^{4,12,18,19,22,33,35}. Trained cells have been shown to display certain characteristics including enhanced cytokine recall response, enhanced protection against heterologous infections as well as epigenetic and metabolic modifications^{20,82}. Overall, the field has a strong understanding of how systemic exposure to various agents can give rise to trained innate immune cells and its underlying mechanisms. On the other hand, knowledge regarding how local mucosal exposure to different agents may result in the training of innate cells is much more limited⁶.

There are some concerns over maladaptive TII leading to persistent, systemic inflammation and contributing to inflammatory co-morbidities⁸³. It has been shown that periodontitis-induced systemic inflammation can lead to arthritis, and other groups have also raised concerns regarding TII increasing the risk for atherosclerosis^{83–85}. In this regard, we proposed that locally induced, tissue specific TII may have merits over systemically induced TII^{6,32}. Directly targeting the site of infection could counter global imprinting and an immunological bias which may put the host at a disadvantage. To this end, previous work in our lab has shown that acute respiratory mucosal viral infection can induce memory in AMs and TII in the lung. Since besides viruses, the lung may be exposed to other types of infectious agents such as fungi and bacteria, we are interested in assessing the potential effects of respiratory mucosal exposure to a purified microbial component and how

this may compare to a live microbial agent. While β -Glucan has been widely utilized to induce TII in peripheral cells following systemic delivery, little is known about its effects on the induction of innate immune memory in mucosal tissue-resident macrophages following local exposure.

Since this project explored a new model for TII following respiratory mucosal exposure to β -Glucan, it was important to examine commonalities and differences in altered AMs following respiratory mucosal exposure to a live infectious agent vs. a well-defined microbial component. One of the main characteristics of TII is protection against heterologous infections. As previously mentioned, AMs are the first line of defense against *S. pneumoniae* infection, their ability to bind and recognize the pathogen as well as invoke a robust immunological response is crucial to the outcome of infection^{56,57}. Following RM-exposure to an Ad-vectored vaccine, memory AMs have been shown to provide enhanced protection against infection with *S. pneumoniae*³². Since the current project also made use of *S. pneumoniae* as a bacterial infectious model, it allowed for a comprehensive comparison between Ad and β -Glucan-altered AMs regarding their phenotype, functionality as well as protective efficacy against respiratory *S. pneumoniae* infection.

Thus, the **Objective** of this project was to investigate whether respiratory mucosal exposure to a purified microbial component induces memory-like AMs and if so, how these innate memory cells compare to those induced by acute respiratory viral infection in phenotype and capacity to induce TII. Based on our previous work and the current understanding in the field, we **hypothesize** that respiratory mucosal exposure to β -Glucan will induce memory AMs. However, such altered AMs will differ from those induced by acute Ad infection in phenotype, origin, and longevity.

Associated with β -Glucan-induced memory AMs will be enhanced TII against acute, heterologous *S. pneumoniae* infection.

We intend to address our hypothesis via pursuing the following **aims**:

Aim 1) Investigate the effects of respiratory β -Glucan exposure on alveolar macrophages.

Aim 2) Compare β -Glucan and acute Ad infection-induced changes in AMs and protective efficacy against *S. pneumoniae* infection.

1.12 – Project significance

This project serves to further the understanding of innate immune memory and TII in an important barrier tissue site, the respiratory mucosa. This project will also further the understanding of how respiratory mucosal exposure to purified microbial components and live organisms lead to alterations in the lung microenvironment and thus potential immunophenotypic, functional and metabolic changes in the tissue-resident innate immune cells. This field is quite young and such new knowledge has important implications in understanding the mechanisms of mucosal host defense and developing new immunotherapeutic, immuno-adjuvants, and vaccine strategies.

2.0 – Materials and Methods

Mice

Wild-type female Balb/c mice were obtained from Charles River Laboratories (Saint Constant, QC, Canada). All mice utilized were 6 to 8 weeks old upon arrival and housed in either a specific pathogen-free level B or biosafety level 2 facility at McMaster University, Hamilton, ON, Canada. All performed experiments were in accordance with institutional guidelines from the Animal Ethics and Research Board.

Inoculation with fungal cell wall polysaccharide β -Glucan

β -Glucan peptide was obtained from InvivoGen (San Diego, CA, USA). β -Glucan polysaccharide, isolated from *Trametes versicolor* and conjugated to a peptide, was used for all experiments. 50 μ g or 25 μ g of β -Glucan was dissolved in 25 μ L of phosphate buffered saline (PBS) per mouse. Mice were inoculated intranasally with 25 μ L of the mixed solution.

Inoculation with replication-deficient adenoviral-vector

Inoculation was performed with a replication-deficient recombinant human serotype 5 adenovirus expressing a *Mycobacterium tuberculosis* protein Ag85A (AdHu5Ag85A). Previous publications have described the production and utilization of these viruses³². The viral vector was prepared in 25 μ L of PBS with a dose of 5x10⁷ PFU per mouse. All inoculations of this virus were undertaken intranasally with 25 μ L of the virus preparation.

Inoculation with PKH26 dye

For every 10 mice to be inoculated, 10 μ L of PKH26 dye from Sigma Aldrich (St. Louis, MO, USA) [1000 μ M] was added into 90 μ L of 100% EtOH resulting in a concentration of [100 μ M].

From there, 100 μ L of the diluted dye was added into 400 μ L of Diluent B from Sigma Aldrich (St. Louis, MO, USA) resulting in a concentration of [20 μ M]. 50 μ L of this mixture was then intratracheally inoculated into Balb/c mice.

Bronchoalveolar lavage cell isolation

Mice were euthanized by exsanguination and cells for bronchoalveolar lavage (BAL) were isolated as previously described³². Isolated BAL cells were resuspended in either PBS for flow cytometry staining or in complete RPMI 1460 media (RPMI 1460 supplemented with 10% or 2% FBS and 1% L-Glutamine, with or without 1% penicillin/streptomycin) for ex vivo culture. Isolated cells were counted under a microscope using either Turks Blood Dilution Fluid (RICCA Chemical, Arlington, TX, USA) or Trypan Blue 0.4% (Gibco, ThermoFisher Scientific, Waltham, MA, USA).

Cell surface immunostaining

Cell staining and flow cytometry were both performed as has been previously described³². Cells isolated from BAL were plated in U-bottom 96 well plates. Cells then underwent Aqua dead cell staining (ThermoFisher Scientific, Waltham, MA, USA) at room temperature for 30 minutes. Subsequently, cells were washed and then blocked for 15 minutes on ice, with anti-CD16/CD32 (clone 2.4G2) in 0.5% bovine serum albumin-PBS (FACs buffer), the cells were then stained for 30 minutes on ice with fluorochrome-labeled mAbs. The fluorochrome-labeled mAbs utilized for staining were anti-CD45-APC-Cy7 (clone 350-F11), anti-CD11c-APC (clone HL3), anti-CD11b-PE-Cy7 (clone M1/70), anti-MHC II-Alexa Fluor 700 (clone M5/144.15.2) (Thermo-Fisher Scientific, Waltham, MA, USA), anti-CD3-V450 (clone 17A2), anti-CD45R (B220)-V450 (clone

RA3-6B2), anti-Ly6c-Biotin (clone HK1.4), Streptavidin-Qdot800 (Thermo-Fisher Scientific, Waltham, MA, USA), anti-CD24-BV650 (clone M1/69) (BioLegend, San Diego, CA, USA), anti-CD64-PE (clone X54-5/7.1) (BioLegend, San Diego, CA, USA), anti-Ly6G-BV605 (clone 1A8), anti-Siglec-F-PECF594 (clone E50-2440). All fluorochrome-labelled mAbs were obtained from BD Biosciences (NJ, USA) unless otherwise specified. Following BD Biosciences instructions, stained cell samples were processed for flow cytometry. Stained samples were run on a BD LSR II or BD Fortessa flow cytometers. Data was then analyzed using the FlowJo software (version 10.1; Tree Star, Ashland, OR, USA).

Intracellular immunostaining

Isolated BAL cells were plated in a 48-well flat-bottom plate (1.5×10^5 cells/well) in AM media (RPMI 1740 supplemented with 2% FBS, 1% L-glutamine, 1% penicillin/streptomycin, and 1x HEPES) in a total volume of 350 μ L. Cells were rested for 2 hours at 37°C and then checked under a microscope to confirm an evenly distributed monolayer. Cells were then washed twice with PBS, unstimulated samples received 350 μ L of AM media. Stimulated wells received AM media with stimulants added, *M. tuberculosis* WCL [50ng/ μ L] or LPS (Sigma-Aldrich, St. Louis, MO, USA) [50ng/ μ L]. Whole blood samples underwent simpler processing and were plated as is with 200 μ L of sample added to each well. The cells then received received RPMI with stimulants added, *M. tuberculosis* WCL [50ng/ μ L] or LPS [50ng/ μ L]. The plates were incubated in a 37°C, CO₂ incubator. After 3 hours, 50 μ L of Golgiplug (BD Biosciences, NJ, USA) protein transporter inhibitor (1:100 in AM media or RPMI) was added to each well and plates were incubated overnight in a 37°C, CO₂ incubator. The following day, AMs were lifted from the bottom of the 48-well flat-bottom plate by rinsing once with PBS and then FACS buffer, cells were then rested

on ice for 20 minutes. Cells were released from the bottom by gently tapping or using the bottom of a pipette tip to gently scrape at the end, transfer the samples into a 96 well U-bottom plate and centrifuged at 1400 for 5 minutes. Both AMs and whole blood cells then underwent Aqua dead cell staining (ThermoFisher Scientific, Waltham, MA, USA) at room temperature for 30 minutes. Cells then underwent Cytotfix/Cytoperm™ staining (BD Biosciences, NJ, USA). Subsequently, cells were washed and then blocked for 15 minutes on ice, with anti-CD16/CD32 (clone 2.4G2) in perm wash buffer (BD Biosciences, NJ, USA). Cells were then stained for 30 minutes on ice with fluorochrome-labeled mAbs. The fluorochrome-labeled mAbs utilized for staining were anti-CD45-APC-Cy7 (clone 350-F11), anti-CD11c-APC (clone HL3), anti-CD11b-PE-Cy7 (clone M1/70), anti-MHC II-Alexa Fluor 700 (clone M5/144.15.2) (Thermo-Fisher Scientific, Waltham, MA, USA), anti-CD3-V450 (clone 17A2), anti-CD45R (B220)-V450 (clone RA3-6B2), anti-Ly6c-Biotin (clone HK1.4), Streptavidin-Qdot800 (Thermo-Fisher Scientific, Waltham, MA, USA), anti-CD24-BV650 (clone M1/69) (BioLegend, San Diego, CA, USA), anti-IL-6-PE (clone MP5-20F3), anti-Ly6G-BV605 (clone 1A8), anti-Siglec-F-PECF594 (clone E50-2440) and anti-TNF- α -Percp-cy5.5 (clone MP6-XT22). All antibodies were obtained from BD Biosciences unless otherwise stated. Per BD Biosciences instructions, stained cell samples were processed for flow cytometry. Stained samples were run on a BD LSR II or BD Fortessa flow cytometers. Data was then analyzed using the FlowJo software (version 10.1; Tree Star, Ashland, OR, USA).

Respiratory infection with *S. pneumoniae*

As previously described, a clinical isolate of *Streptococcus pneumoniae* (Serotype 3; ATCC 6303; ATCC, Manassas, VA, USA) was used for the respiratory infection model^{32,86}. Frozen bacterial stock was plated on tryptic soy agar plates (BD Biosciences, San Jose, CA, USA) which were

supplemented with 5% defibrinated sheep blood (Hemostat, Dixon, CA, USA) and 10 μ g/ml neomycin (Sigma-Aldrich, St. Louis, MO, USA). The blood agar plates were then incubated in a 5% CO₂ incubator at 37°C for no more than 8 hours. Colonies from the plates were then cultured at 37°C in 5% CO₂ in Todd Hewitt Broth (BD Biosciences, San Jose, CA, USA) to mid-logarithmic phase. Bacteria was harvested and subsequently resuspended in PBS, the infectious dose was confirmed by performing and plating 10-fold serial dilutions on blood agar plates. Mice were then infected, via intratracheal administration, with either 5x10⁴ or 5x10⁵ colony forming units (CFU) of *S. pneumoniae* in 40 μ l of PBS.

Assessment of survival, clinical conditions, and weight loss following S. pneumoniae infection

Following bacterial infection, mice underwent daily monitoring for clinical conditions and body weight loss as previously described³². Moribund mice were terminated and the end point in these experiments was defined as 20% body weight loss from the initial weight or significant clinical illness. Otherwise, mice were sacrificed at experimentally defined time points. Mice were monitored for 5 days post-infection (dpi), all surviving mice at 5dpi were euthanized.

Evaluation of bacterial control following S. pneumoniae infection

To evaluate bacterial control, bacterial CFU assays were performed. Lung and spleen tissues were homogenized in homogenization buffer (PBS supplemented with 10% glycerol and 0.1% Tween80). Tissue homogenates underwent serial dilutions and then were plated on blood agar plates and incubated overnight at 37°C in 5% CO₂. Colonies were counted and calculated as CFU/organ.

Ex vivo phagocytosis and killing assay

This assay was conducted using the same methods as previously described by Yao et al., 2018³². AMs isolated from BAL were resuspended in AM media (RPMI 1740 supplemented with 2% FBS, 1% L-glutamine, 1% penicillin/streptomycin, and 1x HEPES). Cells were then plated in a 48 well flat-bottom plate (250µL/well) at a concentration of [1x10⁵ cells/well]. Cells were incubated at 37°C in a 5% CO₂ cell-culture incubator for two hours. Concurrently, *S. pneumoniae* was grown to optimal OD as described above. Serum from each group was separately added into the bacterial stock and vials were placed into the 5% CO₂ cell-culture incubator for 30 minutes to allow for bacterial opsonization. Bacterial stock was then added to each sample well and the plate was incubated again for 1 hour. Following this, cells were incubated on ice for 30 minutes to halt phagocytosis and cells were subsequently washed with PBS to remove excess bacteria. The killing assay plate was re-incubated for an additional 2 hours to allow for the completion of the killing assay and the phagocytosis plate was prepared for serial dilution plating. At the end of each assay, the plate was washed with PBS and subsequently 200µL of distilled H₂O was added into the sample wells. Cells were then burst by being spun in a centrifuge at 1800 rpm for 3 minutes. Supernatant was removed and after performing serial dilutions was plated on blood agar plates and colonies were counted 12 hours later.

3.0 – Results

3.1 – Respiratory mucosal delivery of adenoviral-vectored vaccine gives rise to memory AMs

To establish and verify technical competence, we first set out to replicate results seen in our previous study where a single respiratory mucosal exposure to a replication-deficient adenovirus-vectored vaccine (AdAg85A or Ad) led to the generation of autonomous memory AMs³². BALB/c mice, 6–8-week-old were inoculated via the intranasal (**i.n**) route with Ad. A set of mice were also inoculated with 25ul of sterile PBS (**naïve**). BAL fluid was collected for mononuclear cell isolation at 14 days post-vaccination (**Figure 1A**). Cells were immunostained and subjected to flow cytometry analysis, using an extensive gating strategy AMs were identified as Ly6G⁻, CD11b⁻, CD11c^{HI}, CD64^{HI}, Ly6C⁻, Siglec-F^{HI}(**Supplementary Figure 1**). Expression intensity of MHC II by AMs was determined as a measure of median fluorescence intensity (MFI). In line with our previous observations, pulmonary exposure to Ad resulted in recruitment of interstitial macrophages (IMs) into the airways as indicated by the Siglec-F⁻,Ly6C⁻ population (**Figure 1B**)³². Pulmonary exposure to Ad also led to increased expression of MHC II on AMs (**Figure 1C**).

3.2 – Inflammatory cellular responses in the airways following intranasal delivery of a low dose or high dose of β -Glucan

We assessed the optimal dose of β -Glucan delivery for the induction of TH1 in tissue-resident AMs following intranasal exposure. The main criteria for an optimal dose were that it must be safe and induce significant alterations to the airways including cellular influx and/or phenotypic changes to airway macrophage populations. Given that our model is of respiratory mucosal exposure and β -Glucan is a highly proinflammatory agent, rather small doses were

chosen. In a systemic exposure study, 1mg of β -Glucan was delivered via intraperitoneal injection³³. We chose to intranasally (**i.n**) deliver either a low dose (LD) 25 μ g or a high dose 50 μ g (HD) of β -Glucan covalently linked to a polypeptide chain. Balb/c mice, 6-8 weeks old were inoculated (**i.n**) with either 25 μ g or 50 μ g of β -Glucan in 25 μ L of PBS. A set of mice were also inoculated with 25 μ L of sterile PBS (**naïve**). Mice were monitored to assess clinical signs of illness including appearance, physical signs (respiration, wounds, diarrhea, and bloody feces), body condition and behaviour. BAL was collected for mononuclear cell isolation at 7 days post-exposure (**Figure 2A**). Cells were immunostained and subjected to flow cytometry analysis according to an extensive gating strategy (**Supplementary Figure 1**). Both doses (25 μ g and 50 μ g) of β -Glucan were found to be safe for intranasal exposure as mice in both groups did not exhibit any overt clinical signs of illness (data not shown). We noted that both LD and HD of β -Glucan, but more prominently, mice receiving HD of β -Glucan had increased total cell numbers in airways compared to naïve counterparts (**Figure 2B**). Such increase in total cells was not accompanied by neutrophils recruitment to the airways (**Figure 2C**). Similarly, total numbers of AMs in the airways did not differ between naïve and β -Glucan exposed animals (**Figure 2D**). Interestingly, we noted an influx of IMs into the airways of β -Glucan exposed mice (**Figure 2F**). This influx was much more pronounced in the HD β -Glucan group. Both LD and HD exposure led to influx of CD3+ T cells into the airways however, such influx was much more substantial in the HD group than in the LD group (**Figure 2E**). Overall, the HD of β -Glucan was safe and induced more cellular influx and alterations to the airway macrophages compared to the LD of β -Glucan. Hence, all following experiments utilized the HD of β -Glucan.

3.3 – Significant and persistent alterations in the airway cellular profile and macrophage phenotype at various timepoints post-intranasal delivery of β -Glucan

We next set out to further evaluate the effects of intranasal β -Glucan delivery on the airway cellular profile and airway macrophage phenotype. It was of particular interest to map out these changes by assessing the cellular profile at multiple time points. In our Ad vaccine model, Ad-induced memory AMs persisted up to 16 weeks post-exposure³². Hence, we were also particularly interested in the longevity of any changes that β -Glucan induced in airways. Mice were inoculated (**i.n**) with 50 μ g of β -Glucan and another set of mice were inoculated with 25 μ l of sterile PBS (**naïve**). BAL fluid was collected 3-, 7-, 14-, 21-, 28- and 56- days post-exposure and flow cytometry was performed (**Figure 3A**). At 3 days post-exposure to β -Glucan there were a significant influx of monocyte-derived macrophages (Ly6c^{hi} and Siglec-F⁻) and interstitial macrophages (Ly6C⁻ and Siglec-F⁻), a significant increase in the total cell numbers, and a large influx of neutrophils in the airways (**Figure 3C and 3F**). By 7 days post-exposure, while a significantly elevated cell count remains, there was a complete loss of the neutrophil population and a significant influx of CD3⁺ T cells into the airways (**Figure 3C and E**). The significant population of CD3⁺ cells seen in the airways 7 days post-exposure, diminished by day 14, which coincided with contraction in total cell numbers (**Figure 3B & 3E**). Total cell numbers in airways returned to baseline by day 28 post-exposure (**Figure 3B**). Furthermore, absolute cell numbers of AMs were quite similar in naïve and β -Glucan-exposed mice (**Figure 3D**). In line with previously described observations, at day 7 post-exposure there was a significant influx of IMs (CD11b^{hi} and Siglec-F⁻) into the airways. At this timepoint, the airway was populated with AMs and IMs and by day 14 post-exposure, in addition to IMs and AMs, a new population which displayed lower Siglec-F expression (SF^{lo}) was found in the airways of β -Glucan exposed animals (**Figure 3F &**

3G). This new population also displayed CD11b⁺ expression that was much higher than in bona fide AMs (**Figure 3G**). Hereafter, this CD11b⁺Siglec-F^{lo} cell population is referred to as Transitioning AMs (Trans AMs). By day 21 post-exposure, the presence of the bona fide IMs further diminished, concurrently the Trans AM population now lacked CD11b⁺ surface expression (similar to bona fide AMs) but still maintained lower levels of Siglec-F when compared to AMs (**Figure 3F & 3H**). The SF^{lo} AM population persisted at d28 co-existing with bona fide AMs (**Figure 3F**). Furthermore, a slightly reduced, but still prominent population of SF^{lo} AMs was still visible up to d56 post-exposure. It is important to note that in naïve airways there were limited AMs that seem to express lower levels of Siglec-F, the population was much reduced in comparison to β -Glucan-exposed (Supplementary Figure 2). Furthermore, they do not display any similar changes seen following β -Glucan exposure including upregulation in CD11b expression (Supplementary Figure 2). Going forward, we did not distinguish AMs with lower Siglec-F expression, from naïve bona fide AMs. Taken together, we can conclude that intranasal exposure to β -Glucan results in the influx of IMs into the airways and significant immunophenotypic changes to the airway macrophages, generating a SF^{lo} AM population by day 21 which were maintained up to day 56 post-exposure.

3.4 – Time-dependent upregulation of MHC II expression in airway macrophages following intranasal delivery of β -Glucan

We next set out to evaluate whether β -Glucan exposure affects MHC II expression levels in AMs, as we have previously documented MHC II expression to be a reliable signature of memory AMs³². Intranasal exposure to β -Glucan led to a time-dependent increase in MHC II expression by bona fide AMs, peaking at day 14 before eventually decreasing to a level comparable

to naïve by day 28 (**Figure 4A**). Trans AMs exhibit a similar upregulation of MHC II expression at day 14 and SF^{lo} AMs exhibit the same at day 21 and 28 (**Figure 4B**). In conclusion, along with immunophenotypic changes in expression of surface markers such as Siglec-F and CD11b (previous experiment), β -Glucan also causes alterations in the expression of MHC II. However, whether these phenotypic changes accompany functional re-programming is yet unclear and has been addressed in later experiments.

3.5 – Significant recruitment and differentiation of circulating monocytes to bona fide AMs following intranasal delivery of β -Glucan

Having characterized the effects of intranasal β -Glucan exposure on the cellular composition of airways and on the AM phenotype, we next investigated the relative contribution of circulating monocytes to the genesis of persisting AM populations following β -Glucan exposure. A recent study utilized the stable fluorescence PKH26 dye to label tissue-resident AMs in the lung⁸⁷. They showed that PKH26 dye can be used to distinguish between bona fide AMs (defined as Siglec-F^{hi}Ly6C-CD11b-) and incoming monocytes that may differentiate into AMs following inflammatory insult. Mice were inoculated (**i.t**) with PKH26 dye, 48 hours post-exposure mice were given either their usual dose of 50 μ g of β -Glucan or 25 μ L of PBS (**naïve**), and then sacrificed at 3-, 14- and 28-days post- β -Glucan exposure (**Figure 5A**). A set of PKH26 treated animals were left unexposed to any other agents (PKH+AM) as a positive control and a set of animals were left untreated with PKH (PKH-AM) as a negative control. At designated timepoints airway cells obtained by BAL were immunostained and subjected to flow cytometry. Dilution/loss of PKH within airway macrophages was calibrated as a measure of MFI of PKH signal.

As expected, prior to β -Glucan exposure the majority of bona fide AMs were labelled with PKH (**Figure 5B**). 3 days post-exposure, majority of bona fide AMs maintained high levels of PKH expression comparable to the positive control. On the contrary, by day 14 there was a considerable dilution of PKH on bona fide AMs, indicating that monocytes recruited to the inflamed lung differentiated and contributed to the bona fide AM pool (**Figure 5B**). By day 28, a fraction of original bona fide AMs still persisted, as indicated by the PKH signal (**Figure 5B**).

Given that there was a unique transitioning population of AMs (Trans AM-Siglec-F^{lo}Ly6C-CD11b+) following intranasal exposure to β -Glucan, we next investigated the genesis of this population. Intriguingly, Trans AMs that emerged by 14 days post-exposure were also positive for PKH, indicating that Trans AMs were derived from the bona fide AM pool that existed prior to β -Glucan exposure, by gaining CD11b surface marker expression (**Figure 5B**). Importantly, the intensity of PKH signal in this population was considerably elevated compared to the positive control (PKH+AM), this raises the possibility that Trans AMs were actively phagocytosing free floating PKH dye molecules released by necrotizing bona fide AMs.

Together, the above data provide evidence for a significant recruitment and differentiation of circulating monocytes to bona fide resident AMs beginning 3 days after β -Glucan exposure.

3.6 – Cytokine production by Ad vaccine- or β -Glucan-trained airway macrophages in response to ex vivo re-stimulation with inflammatory agents

Since one of the hallmarks of TII is enhanced cytokine recall responses by trained innate immune cells, we next set out to assess if β -Glucan exposure-altered AMs would display similar characteristics.^{6,20,31,32} Mice were inoculated (**i.n**) with β -Glucan, Ad or 25ul of PBS (**naïve**) (**Figure 6A**). As a control, we also decided to include a group of mice that received the Ad-

vectored vaccine. 28 days following initial treatment, mice were sacrificed, BAL was obtained, and mononuclear cells isolated and plated in each well and further stimulated with either *Mtb* whole cell lysate (WCL) [50ng/ μ L] or LPS [50ng/ μ L] for 18h (**Figure 6A**). Following stimulation, cells underwent intracellular flow cytometric staining and analysis.

Following an 18h stimulation with WCL, both Ad and β -Glucan-exposed animals exhibited significantly higher frequencies of IL-6+ AMs when compared to naïve counterparts (**Figure 6B**). Interestingly, following WCL stimulation all treatment groups had similar frequencies of TNF- α + AMs (**Figure 6C**). Similarly, following 18h of stimulation with LPS, both Ad and β -Glucan-exposed mice had significantly higher frequencies of IL-6+ AMs when compared to naïve (**Figure 6D**). The frequencies of TNF- α + AMs were similar among naïve and β -Glucan in response to LPS stimulations however, frequencies of TNF- α + Ad-induced memory AMs were lower (**Figure 6E**). Both Ad-induced memory AMs and β -Glucan-altered AMs displayed similar cytokine recall responses secondary stimulations. Given the enhanced functionality and key phenotypic changes associated with TII observed in AMs exposed to β -Glucan, going forward we have labelled these AMs as trained, all the while continuing to accumulate evidence to strengthen this claim. In conclusion, β -Glucan-trained AMs exhibit long-lasting functional enhancements in the form of boosted cytokine recall responses.

3.7 – Changes in circulating monocytes following intranasal delivery of β -Glucan

It was also of interest for us to evaluate the effect of a single respiratory-mucosal exposure to β -Glucan or Ad vaccine on circulating monocytes. To assess this, blood was collected from the abdominal artery of accordingly inoculate mice and was cultured with either WCL [50ng/ μ L] or

LPS [10ng/ μ L] for 18h (**Figure 7A**). Cells then underwent intracellular flow cytometric staining and analysis (**Figure 7A**).

Ly6C^{hi} monocytes from β -Glucan-exposed mice expressed higher levels of MHC II at resting state (**Figure 7B**). Interestingly, following secondary stimulation with either WCL or LPS, Ly6C^{hi} monocytes from both naïve and Ad-exposed mice increased MHC II expression whereas expression levels in β -Glucan-exposed stimulated Ly6C^{hi} monocytes was similar to unstimulated Ly6C^{hi} monocytes (**Figure 7B**). In the absence of stimuli, higher levels of β -Glucan-exposed Ly6C^{hi} monocytes were IL-6⁺ when compared to naïve and Ad Ly6C^{hi} monocytes (**Figure 7C**). WCL or LPS stimulation led to an increase in frequencies of both naïve and Ad IL-6⁺ and TNF- α ⁺ Ly6C^{hi} monocytes positive when compared to unstimulated cells (**Figure 7C and D**). β -Glucan-exposed Ly6C^{hi} monocytes did not exhibit similarly increased frequencies of IL-6⁺ and TNF- α ⁺ following stimulations with either inflammatory agent (**Figure 7D**). β -Glucan-exposed Ly6C^{hi} monocytes displayed some phenotypic shifts marked by increased expression of MHC II and at baseline seemed to have a pro-inflammatory signature (**Figure 7**). However, β -Glucan-exposed Ly6C^{hi} monocytes exhibited a muted response to secondary stimulation. Interestingly, a single intranasal delivery of β -Glucan caused long lasting changes in AMs as well as Ly6C^{hi} monocytes. Nevertheless, the mechanism by which β -Glucan caused these changes and functional/potential training outcomes in Ly6C^{hi} monocytes remains to be investigated.

3.8 – Assessment of bacterial phagocytosis and killing by β -Glucan-trained airway macrophages

We set out to further characterize the functional profile of β -Glucan-trained AMs. Ad-induced memory AMs exhibited enhanced phagocytic and killing capacity, hence a phagocytosis

and killing assay was performed to evaluate the same in β -Glucan-trained AMs. Mice were intranasally inoculated (**i.n**) with either β -Glucan or PBS (**naïve**). 28 days following initial treatment, mice were sacrificed, BAL obtained, and mononuclear cells isolated. Live cells were plated, rested, and then *ex vivo* infected with live *S. pneumoniae*. Cells underwent phagocytic and killing assays, concluding with the assessment of bacterial CFU (**Figure 8A**).

AMs exposed to β -Glucan displayed enhanced phagocytic activity (**Figure 8B**). β -Glucan-exposed AMs phagocytosed significantly more bacteria than naïve AMs, a difference of almost 2-3 log₁₀ (**Figure 8B**). Results from the killing assay suggested that both naïve and β -Glucan-exposed AMs were able to clear 100% of the bacteria (**Figure 8C**). In conclusion, β -Glucan-trained AMs exhibit enhanced phagocytosis, which is another significant functional enhancement.

3.9 – Differential airway cellular responses to intranasal delivery of β -Glucan and Ad-vectored vaccine

Thus far, a significant knowledge gap exists regarding similarities/differences between training by intranasal delivery of a live infectious agent and a purified microbial component. Having seen similar functional enhancements in cytokine recall responses in both β -Glucan-trained AMs and Ad-induced memory AMs, we next set out to compare effects of intranasal exposure to β -Glucan and Ad on the airway cellular responses and AM phenotype (**Figure 6**). Mice were inoculated (**i.n**) with β -Glucan, Ad or PBS (**naïve**). BAL cells were isolated at 14- and 28- days post-exposure subsequently, cells were immunostained and subjected to flow cytometry as done in earlier experiments (**Figure 9A**).

Cell numbers in the airways at 14 days post-exposure were significantly elevated in Ad-exposed mice compared to naïve (**Figure 9B**). β -Glucan-exposed mice showed some elevation in

total cell numbers at day 14 when compared to naïve hosts, but markedly less than Ad-exposed mice (**Figure 9B**). By day 28, both Ad and β -Glucan-exposed mice experienced a contraction in total cell numbers (**Figure 9B**). Absolute cell numbers of AMs in BAL at day 14 and 28 were similar across the three groups (**Figure 9C**). Mice exposed to Ad showed a significant influx of IMs and MDMs at day 14 (**Figure 9D**). β -Glucan exposure also resulted in an influx of IMs when compared to naïve at day 14, but not as robust as seen following Ad exposure (**Figure 9D**). Interestingly, the Trans AM population (defined as SF^{lo} and $CD11b^+$) seems to be present in both Ad and β -Glucan-exposed mice at day 14 post-exposure with the population being much more prominent in the β -Glucan-exposed mice (**Figure 9D**). Furthermore, at 14 days post-exposure, Ad-exposed mice had a MDM population in the airways which was lacking in other groups (**Figure 9D**). By 28 days post-exposure, both Ad and β -Glucan-exposed mice underwent further cellular profile alterations in the airways. Ad-induced influx of MDM and IM populations diminished by 28 days leaving Ad-exposed mice with mostly a bona fide AM population along with some TransAMs (**Figure 9D**). In contrast, by 28 days, β -Glucan-exposed SF^{lo} AMs co-existed with bona fide AMs. This SF^{lo} AM population was unique to β -Glucan-exposed mice and was not present at this timepoint following Ad exposure (**Figure 9D**). Furthermore, intranasal exposure to Ad resulted in a significant increase in the MFI of MHC II at both 14- and 28-days post-exposure when compared to naïve and β -Glucan (**Figure 9E and F**). In conclusion, inflammatory responses in the airways following Ad vaccine and β -Glucan exposure differ considerably.

3.10 – TII elicited by intranasal delivery of β -Glucan or Ad-vectored vaccine provides enhanced protection against clinical outcomes from heterologous *S. pneumoniae* infection

Enhanced protection against a secondary heterologous infection is a hallmark of TII^{6,32}. In this model we utilized a live infection with *S. pneumoniae*, as previously undertaken in the Ad model³². Mice were intranasally inoculated with β -Glucan, Ad or PBS (**naïve**). 28 days later, mice were challenged with a lethal dose of *S. pneumoniae* (5×10^4 CFU). Clinical outcomes including body weight changes, signs of illness (appearance, respiration, wounds, diarrhea and bloody feces, body condition and behaviour), and survival rates were monitored for 120 hours post-infection (**Figure 10A**).

Following challenge with a lethal dose of *S. pneumoniae*, 50% of naïve mice died by 72 hours post-infection, whereas only 10% of the β -Glucan-exposed mice and none of the Ad-exposed mice had succumbed to infection (**Figure 10C**). By the completion of the experiment, only 30% of naïve mice were surviving, whereas around 70% of β -Glucan and Ad-exposed mice survived (**Figure 10C**). Furthermore, by 120 hours post-infection naïve mice lost significantly more weight than β -Glucan and Ad-exposed mice (**Figure 10B**). Finally, when mice were scored for signs of illness, Ad-exposed mice had significantly lower clinical scores when compared to naïve (**Figure 10C**). β -Glucan-exposed mice had slightly higher scores than Ad-exposed mice and slightly lower than naïve mice, but this was not statistically significant (**Figure 10C**). Overall, protective capacity against lethal *S. pneumoniae* infection was comparable between β -Glucan and Ad-exposed mice.

3.11 – TII elicited by intranasal delivery of β -Glucan or Ad-vectored vaccine provides enhanced control of *S. pneumoniae* infection in the lung

We further assessed the capacity for β -Glucan and Ad exposure to induce enhanced control of bacterial CFU. Mice were inoculated (**i.n**) with β -Glucan, Ad vaccine or PBS (**naïve**). Mice were subsequently challenged with a lethal dose of *S. pneumoniae* (5×10^4 CFU) and sacrificed 72 hours post-infection. After sacrifice, blood, spleen, and lung were collected and bacterial CFU was assessed (**Figure 11A**). Due to issues with virulence of *S. pneumoniae*, a lethal dose from a newly obtained vial of *S. pneumoniae* of the same source and serotype was determined. The new lethal dose was established as 5×10^5 CFU of *S. pneumoniae* and similarly, mice were sacrificed 72 hours post-infection, spleen and lung were collected for bacterial CFU, weight loss and clinical signs of illness were also monitored in this experiment (**Figure 12A**).

When compared to naïve, both Ad and β -Glucan-exposed mice exhibited significantly lower bacterial burden in the lung (**Figure 11B**). Results from spleen and blood CFU had quite some variation between different groups and the systemic assessment did not allow for any concrete conclusions (**Figure 11C & 11D**). Such experimental set up was repeated in the model with the newly established lethal dose for *S. pneumoniae* infection (5×10^5 CFU/mouse) (**Figure 12A**). Although not statistically significant, there was an appreciable level of decrease in bacterial CFU in the lung of β -Glucan-exposed mice when compared to their naïve counterparts (**Figure 12B**). Interestingly, spleen from β -Glucan-exposed mice had significantly less bacterial CFU in comparison to naïve counterparts (**Figure 12C**). No differences in weight loss or clinical scores between the naïve and β -Glucan-exposed mice were observed (**Figure 12D**). It is evident that both Ad and β -Glucan-exposed mice can better control *S. pneumoniae* infection in the lung to a similar degree. β -Glucan-exposed mice also displayed enhanced control of *S. pneumoniae* infection in the

periphery. β -Glucan exposure allows for enhanced protection against a secondary heterologous bacterial infection, and this is another strong piece of evidence indicative of TII in this model. However, the specific contribution of AMs and mechanisms for this protection remains to be investigated.

3.12 – Differential airway immune responses to *S. pneumoniae* infection following intranasal delivery of β -Glucan and Ad-vectored vaccine

We next set out to examine airway immune responses following lethal challenge with *S. pneumoniae*. Mice were inoculated with their respective agents and 28 days later challenged with a lethal dose of *S. pneumoniae* (5×10^4 CFU). Mice were sacrificed at 18- or 36-hours post-infection, BAL was collected, immunostained and subjected to flow cytometric analysis (**Figure 13A**). 18h post-infection, there was a significant increase in the total cells in airways of Ad-exposed mice, while cell numbers in naïve and β -Glucan-exposed mice remained stable (**Figure 13B**). By 36h post-infection, total cell numbers in Ad-exposed mice contracted to a similar level as pre-infection (**Figure 13B**). Total cell numbers in the naïve group increased at 36h compared to 18h post-infection, and in β -Glucan-treated mice, cell counts were slightly decreased (**Figure 13B**).

Neutrophils play an important role in the immune response against *S. pneumoniae* and enhanced neutrophilia is key to the boosted protection provided by Ad memory AMs³². In line with previously published data, Ad-exposed mice exhibited a significant increase in neutrophilia at 18h post-infection which contracted by 36h post-infection (**Figure 13C, D, E & F**). At 18h post-infection, such enhanced early-phase neutrophilia was absent in naïve and β -Glucan-exposed mice (**Figure 13C, E & F**). By 36h post-infection, increased neutrophilia contracted in Ad-exposed mice, simultaneously a significant increase in neutrophilia was observed in the naïve group

(**Figure 13D, E & F**). Neutrophil presence in β -Glucan-exposed mice was slightly increased by 36h post-infection but considerably lower than naïve (**Figure 13D, E and F**). In the case of AMs, both absolute numbers and frequency of live observed a significant decrease in all 3 groups and these numbers did not rebound by 36h (**Figure 13 G and H**). Flow cytometric analyses of the two different time points 18h (**Figure 13C**) and 36h (**Figure 13D**) corroborated the information described above. While neutrophil populations underwent changes, it is of note that phenotypes/population frequencies of macrophages did not undergo significant alterations between 18h and 36 h post-infection (**Figure 13C & D**). In conclusion, while enhanced early-phase neutrophilia is a key mechanism for protection in the Ad TII model, in the β -Glucan model, similar early-phase neutrophilia is not detected. Thus, although the exact mechanism behind β -Glucan-exposure induced enhanced protection against acute *S. pneumoniae* infection remains to be investigated. We hypothesize that protection in this model may be dependent on enhanced phagocytosis and increased pro-inflammatory cytokine secretion as noted in earlier experiments (**Figures 6 & 8**).

4.0 – Discussion

For decades, the field of immunology has abided by the dichotomy of the innate and adaptative immune system having their own specific characteristics. One of the main documented differences is that only the adaptive immune system was believed to possess the capacity to form memory against encountered antigens/pathogens⁶. From an evolutionary perspective, it is known that only ~3% of organisms on Earth possess adaptive immunity whereas the other 97% rely solely on the innate immune system⁸². It has been well-established that plants and invertebrates, although lacking an adaptive immune system, can display adaptive immunity-like characteristics^{88,89}. Following exposure to an infectious agent, through epigenetic modifications, these organisms displayed enhanced protection upon exposure to the same or a different infectious agent⁶. Non-specific protection is a hallmark of TII and has not only been observed in invertebrates and plants, but also in humans and other mammals. Vaccines such as BCG have displayed non-specific cross protective effects^{11,12,16,18,19,90}. BCG has been studied extensively and been shown to be a potent agent for the induction of TII in both clinical and pre-clinical studies. Other than BCG, the OPV and MMR vaccine have also been associated with non-specific trained immunity in human populations⁸. Although young, the field of TII has uncovered crucial knowledge about human health and disease and is full of unexplored avenues that could have major implications in therapeutics and vaccine strategies.

Besides vaccines, inflammatory agents of all kinds, ranging from live wild-type organisms to purified inflammatory molecules, have been documented in their varying capacities to induce TII. The most popular training agents in the field include BCG, LPS and β -Glucan which have been extensively studied in their capacity to induce TII in various models following systemic exposure⁶. Our lab established the phenomena of local training of tissue resident AMs following respiratory mucosal exposure to a replication-deficient adenovirus³². Given the ample knowledge

of induction of TII following systemic β -Glucan exposure, we set out to assess the potential for training of airway tissue-resident AMs following respiratory mucosal exposure to β -Glucan and how it would compare to live viral infection.

We found that a dose of 50 μ g/mouse of β -Glucan was safe for intranasal exposure and induced a robust immune response in the airways (**Figure 2**). 3 days post-exposure we saw a large influx of MdMs and IMs into the airways and by 7 days post-exposure, β -Glucan further altered the cellular profile of the airways. There was a substantial influx of T Cells into the airways and significant alterations to the airway macrophage populations (**Figure 3**). Exposure to β -Glucan led to further immunophenotypic alterations to the populations of macrophages in the airways with the appearance of Trans AMs at day 14, and SF^{lo} AMs at day 21 which were maintained until 8 weeks post-exposure (**Figure 3**).

Furthermore, intranasal exposure to β -Glucan was shown to significantly upregulate MHC II expression on bona fide AMs, Trans AMs and SF^{lo} AMs (**Figure 4**). As we previously reported, upregulation of MHC II was one of the key characteristics of Ad-induced memory AMs³². Interestingly, we are not the only group to have seen an increase in MHC II on AMs during training, multiple groups have reported this as a outcome of training in AMs^{69,91}. Of note, in both of the aforementioned studies, trained AMs also exhibited a decrease in Siglec-F expression following training, strengthening the claim that the phenotypic shifts we have seen in the β -Glucan model are associated with training. It is clear that intranasal exposure to β -Glucan changes the cellular profile of the airways and significantly alters the phenotype of airway macrophage subsets in a way similar to other training agents used in the field.

Many of the models of training in the field have shown that monocytes play a very important role in trained innate immunity^{1,23,26,42,69,92}. On the other hand, we have found no

contribution of monocytes to the Ad-induced memory AMs³². Hence it was pertinent for us to further investigate the relative contribution of monocytes in the responses and alterations seen following intranasal exposure to β -Glucan. 3 days post-exposure, there was indeed a significant recruitment of circulating monocytes into the airways following intranasal delivery of β -Glucan and these circulating monocytes further differentiated into bona fide tissue-resident AMs at later timepoints (**Figure 5B**). The contribution of circulating monocytes is certainly key in the immune responses and phenotypic shifts seen following β -Glucan exposure.

It has been well-established that training of innate immune cells accompanies changes in cell functionality. One of the hallmarks of training is an enhanced cytokine recall response upon stimulation with a heterologous agent^{6,16,20,33}. When we assessed functional changes induced in β -Glucan-exposed AMs we found that following secondary stimulation, with either WCL or LPS, AMs had higher frequencies of IL-6⁺ cells (**Figure 6**). This is evidence that indeed β -Glucan-trained AMs display a key characteristic of TII, in the form of enhanced functionality upon secondary stimulation. Furthermore, we observed that a single respiratory-mucosal inoculation of β -Glucan was sufficient to induce alterations to circulating blood monocytes. Although, how and whether these peripheral monocytes may be altered or trained was beyond our current scope of investigation (**Figure 7**). Ad-induced memory AMs exhibited enhanced phagocytic and killing capacity against extracellular heterologous bacteria³². We undertook the same phagocytosis and killing assays to assess enhanced functionality of β -Glucan-trained AMs. β -Glucan-trained AMs indeed exhibited enhanced phagocytosis of bacteria, another key piece of evidence of enhanced functionality associated with TII (**Figure 8**). It is evident that intranasal exposure to β -Glucan causes long lasting phenotypic changes in AMs and these trained AMs exhibit enhanced functionality indicative of TII.

A pressing question that we had was how and if training may differ between exposure to a live organism vs a purified microbial component. To investigate this, we employed our Ad-induced memory AM model for a comparison with trained AMs following β -Glucan exposure³². Intranasal exposure to a live viral agent and a purified microbial molecule induced differential innate responses in macrophage subsets of the airways. (**Figure 9A**). At day 14, there were some similarities between the two responses, namely the influx of IMs and presence of TransAMs. One of the striking differences between Ad and β -Glucan-exposed mice is the presence of MdMs in the Ad-exposed mice at d14 (**Figure 9D**). At day 28, the major difference between the two models was the prominent persistence of SF^{lo} AMs in the β -Glucan model and absence of such a population following Ad exposure (**Figure 9**). Another striking difference between the two models is that β -Glucan-trained AMs receive significant contribution from circulating monocytes whereas Ad-induced memory AMs do not require monocytic contribution (**Figure 5**)³². Indeed, training by these two agents have some similarities in immune responses in the airways, but also key differences in cellular responses and phenotypes of airway macrophages.

A key outcome of trained innate immunity is the capacity for trained cells to contribute to enhanced protection against a secondary heterologous agent⁶. For this investigation we chose to replicate the *S. pneumoniae* challenge model used in experiments our Ad training model³². Both Ad and β -Glucan-exposed mice displayed enhanced rates of survival, minimal body weight loss and reduced bacterial burden in the lung following lethal challenge (**Figure 10**). The first set of challenge experiments indicated similar protective efficacy between Ad and β -Glucan against *S. pneumoniae* infection through enhanced bacterial control in the lung. However, it is important to note that there is a limitation in this data set due to quite some variation within each group (**Figure 11B**). The second set of challenge experiments corroborated the previously seen phenomenon that

β -Glucan exposure enhanced bacterial control in the lung and enhanced control in the periphery was also noted (**Figure 12**). Assessment of the immune response to acute *S. pneumoniae* infection showed that the early-phase enhanced neutrophilia seen in Ad-exposed mice was not present in β -Glucan-exposed mice (**Figure 13**). Late-phase neutrophilia, which can be linked to maladaptive immune responses and immunopathology, was observed only in the naïve group⁹³ (**Figure 13**). Although exposure to Ad and β -Glucan led to markedly distinct responses and airway cellular profiles, both provided similarly enhanced protection against infection with *S. pneumoniae*. In the Ad model, improved protection was associated with enhanced early-phase neutrophilia. On the other hand, in the β -Glucan model there were no significant alterations to the airway cellular profile following *S. pneumoniae* infection, leaving any cellular mechanisms of protection unknown at this time.

Thus far, we have established that intranasal exposure to β -Glucan modulated innate immune responses in the airways and caused long lasting and significant phenotypic alterations to the airway macrophage populations. Associated with these phenotypic alterations and unique macrophage populations was enhanced cytokine secretory capacity following secondary stimulation. Furthermore, β -Glucan-trained AMs exhibited enhanced phagocytic capacity against live *S. pneumoniae*. β -Glucan exposure also provided enhanced protective efficacy against lethal *S. pneumoniae* infection. Enhanced protective efficacy was seen by improved survival, diminished weight loss and augmented control of bacterial CFU in lung and periphery. At this point, specific mechanisms behind the protection seen in this model as well as the specific contribution of β -Glucan-trained AMs remain unknown. However, we can hypothesize that protection in the β -Glucan model may be dependent on enhanced phagocytosis and enhanced pro-inflammatory cytokine secretion as seen in previous experiments under aim 1. Trained AMs generated following

β -Glucan-exposure displayed key characteristics of TII, as summarized in the diagram below. Overall, this project has helped uncover pertinent knowledge regarding innate immune memory and the capacity for locally induced innate immune training at a key mucosal site.

Diagram 1

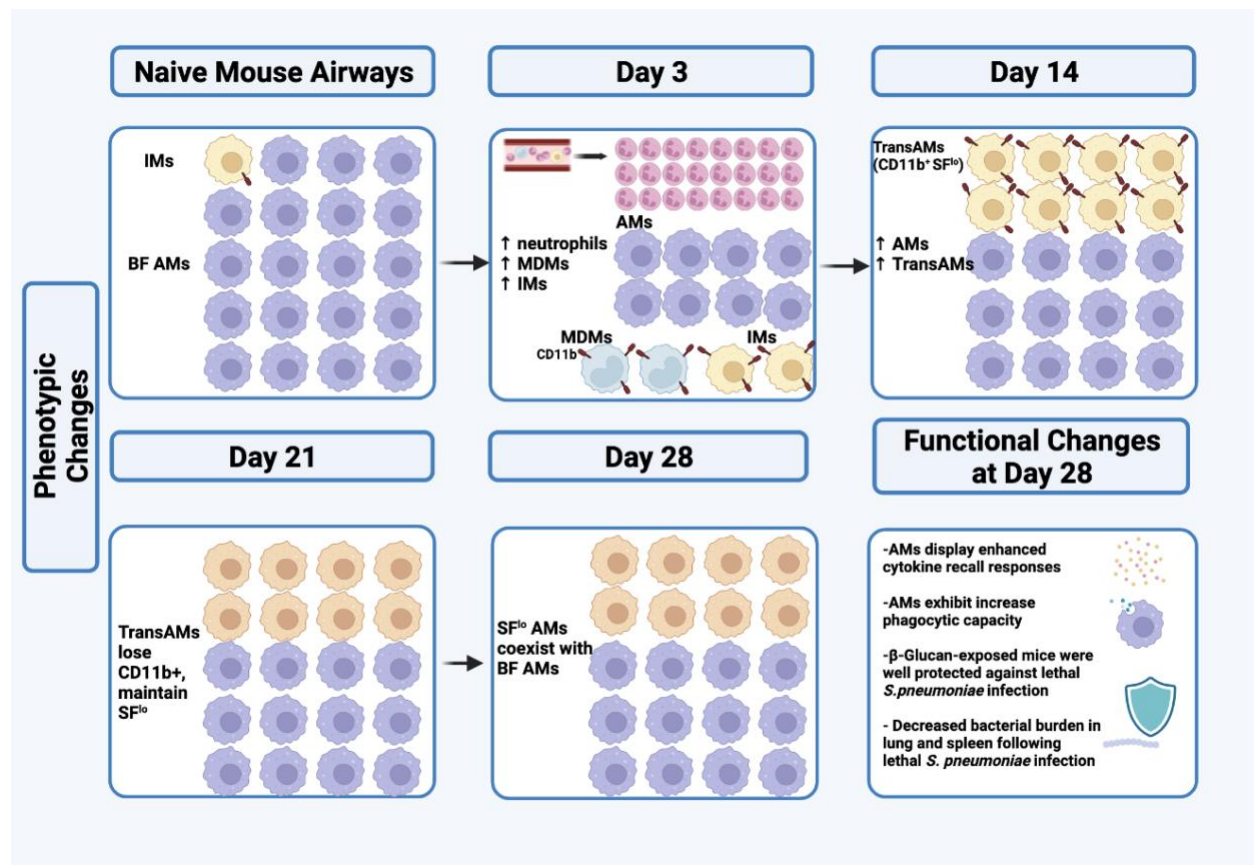


Diagram 1: Conceptual summary of the effects of β -Glucan following intranasal delivery

Future Directions

From all that we have uncovered, two avenues of this project remain to be evaluated and are possible future directions. A full characterization of the metabolic and transcriptomic profile of β -Glucan-trained AMs is needed to assess this key characteristic of TII in this model. Upregulation of glycolysis has previously been characterized in memory-AMs following Ad-exposure^{24,32,42,86}. Therefore, it would be of great interest to perform a seahorse glycolytic assay,

to assess glycolytic capabilities of AMs by measuring the extracellular acidification rate (ECAR) as a function of lactic acid secretion. This assay will allow for the characterization of any TII-indicative metabolic changes occurring in AMs following intranasal β -Glucan exposure. Furthermore, detailed single-cell transcriptomic analyses would help in gaining an overall understanding of which genes may be upregulated in β -Glucan-trained AMs. These experiments would allow for a well-rounded metabolic and transcriptomic profile of β -Glucan-trained AMs.

The second unexplored avenue of this project is to perform an assessment of the specific contribution and mechanisms by which β -Glucan-trained AMs induced TII against *S. pneumoniae* infection. Although exposure to Ad and β -Glucan led to different immune responses, exposure to both was protective against *S. pneumoniae* infection. A sophisticated experimental approach taken by Yao *et al.* has shown that Ad-induced memory AMs, when adoptively transferred into the airways of naïve recipient mice, were still able to enhance protection against *S. pneumoniae*⁴⁶. In the future, an adoptive transfer experiment could be undertaken to ascertain the specific contribution of β -Glucan-trained AMs in enhanced protection against *S. pneumoniae* infection. Another approach to tackle this question could involve the employment of fluorescent *S. pneumoniae* bacteria. This approach would allow for a clear picture of bacterial localization in the airways, helping shed light on how and which cells are interacting with *S. pneumoniae*. Furthermore, usage of monoclonal antibodies to block specific cytokines/receptors could also prove useful in uncovering the mechanism underlying enhanced protection. These two aspects of this project still require further investigation and are important future directions for this project.

5.0 – References

1. Farber, D. L., Netea, M. G., Radbruch, A., Rajewsky, K. & Zinkernagel, R. M. Immunological memory: Lessons from the past and a look to the future. *Nat. Rev. Immunol.* **16**, 124–8 (2016).
2. Medzhitov, R. & Janeway, C. Innate immune recognition: Mechanisms and pathways. *Immunol. Rev.* **Feb**, 89–97 (2000).
3. Bowdish, D. M. E., Loffredo, M. S., Mukhopadhyay, S., Mantovani, A. & Gordon, S. Macrophage receptors implicated in the ‘adaptive’ form of innate immunity. *Microbes Infect.* **Nov-Dec**, 1680–7 (2007).
4. Quintin, J., Cheng, S. C., van der Meer, J. W. M. & Netea, M. G. Innate immune memory: Towards a better understanding of host defense mechanisms. *Curr. Opin. Immunol.* **Aug**, 1–7 (2014).
5. Kurtz, J. Specific memory within innate immune systems. *Trends Immunol.* **26**, 186–92 (2005).
6. Xing Z, Afkhami S, Bavananthasivam J, Fritz DK, D’Agostino MR, Vaseghi-Shanjani M, Yao Y, J. M. Innate immune memory of tissue-resident macrophages and trained innate immunity: Re-vamping vaccine concept and strategies. *J. Leukoc. Biol.* **108**, (2020).
7. Netea, M. G. *et al.* Trained immunity: A program of innate immune memory in health and disease. *Science.* **352**, (2016).
8. Sørup, S., Benn, C. S., Stensballe, L. G., Aaby, P. & Ravn, H. Measles-mumps-rubella vaccination and respiratory syncytial virus-associated hospital contact. *Vaccine* **33**, 237–245 (2015).
9. Stensballe, L. G. *et al.* Acute lower respiratory tract infections and respiratory syncytial virus in infants in Guinea-Bissau: A beneficial effect of BCG vaccination for girls: Community based case-control study. *Vaccine* **23**, 1251–7 (2005).
10. Jeyanathan, M., Yao, Y., Afkhami, S., Smaill, F. & Xing, Z. New Tuberculosis Vaccine Strategies: Taking Aim at Un-Natural Immunity. *Trends Immunol.* **38**, 419–433 (2018).
11. Netea, M. G. & Van Crevel, R. BCG-induced protection: Effects on innate immune memory. *Semin. Immunol.* **26**, 512–7 (2014).
12. Cirovic, B. *et al.* BCG Vaccination in Humans Elicits Trained Immunity via the Hematopoietic Progenitor Compartment. *Cell Host Microbe* **28**, 322-334.e5 (2020).
13. van Puffelen, J. H. *et al.* Trained immunity as a molecular mechanism for BCG immunotherapy in bladder cancer. *Nat. Rev. Urol.* **17**, 513–525 (2020).
14. Bagheri, N. & Montazeri, H. On BCG Vaccine Protection from COVID-19: A Review. *SN Compr. Clin. Med.* **3**, 1261–1271 (2021).
15. Giamarellos-Bourboulis, E. J. *et al.* Activate: Randomized Clinical Trial of BCG Vaccination against Infection in the Elderly. *Cell* **183**, 315-323.e9 (2020).
16. Kaufmann, E. *et al.* BCG Educates Hematopoietic Stem Cells to Generate Protective Innate Immunity against Tuberculosis. *Cell* **172**, 176-190.e19 (2018).
17. Kaufmann, E. *et al.* BCG vaccination provides protection against IAV but not SARS-CoV-2. *Cell Rep.* **38**, (2022).
18. Kleinnijenhuis, J. *et al.* BCG-induced trained immunity in NK cells: Role for non-specific protection to infection. *Clin. Immunol.* **155**, 213–9 (2014).
19. Moorlag, S. J. C. F. M. *et al.* BCG Vaccination Induces Long-Term Functional Reprogramming of Human Neutrophils. *Cell Rep.* **33**, (2020).

20. Quintin, J. *et al.* Candida albicans Infection Affords Protection against Reinfection via Functional Reprogramming of Monocytes. *Cell Host Microbe* **12**, 223–232 (2012).
21. Khan, N. *et al.* M. tuberculosis Reprograms Hematopoietic Stem Cells to Limit Myelopoiesis and Impair Trained Immunity. *Cell* **183**, 752-770.e22 (2020).
22. Camilli, G., Tabouret, G. & Quintin, J. The Complexity of Fungal β -Glucan in Health and Disease: Effects on the Mononuclear Phagocyte System. *Front. Immunol.* **16**, (2018).
23. Mitroulis, I. *et al.* Modulation of Myelopoiesis Progenitors Is an Integral Component of Trained Immunity. *Cell* **172**, 147-161.e12 (2018).
24. Cheng, S. C. *et al.* MTOR- and HIF-1 α -mediated aerobic glycolysis as metabolic basis for trained immunity. *Science*. **26**, 6204 (2014).
25. dos Santos, J. C. *et al.* β -Glucan-Induced Trained Immunity Protects against Leishmania braziliensis Infection: a Crucial Role for IL-32. *Cell Rep.* **28**, 2659–2672 (2019).
26. Moorlag, S. J. C. F. M. *et al.* β -Glucan Induces Protective Trained Immunity against Mycobacterium tuberculosis Infection: A Key Role for IL-1. *Cell Rep.* **31**, (2020).
27. Kalafati, L. *et al.* Innate Immune Training of Granulopoiesis Promotes Anti-tumor Activity. *Cell* **183**, (2020).
28. ShuShun, L. & Christopher, M. β -1,3-glucan induces natural killer cell memory-like immunity. *J. Immunol.* **204**, (2020).
29. Heng, Y. *et al.* Systemic administration of β -glucan induces immune training in microglia. *J. Neuroinflammation* **18**, (2021).
30. Wendeln, A. C. *et al.* Innate immune memory in the brain shapes neurological disease hallmarks. *Nature* **556**, 332–338 (2018).
31. Novakovic, B. *et al.* β -Glucan Reverses the Epigenetic State of LPS-Induced Immunological Tolerance. *Cell* **167**, 1354–1368 (2016).
32. Yao, Y. *et al.* Induction of Autonomous Memory Alveolar Macrophages Requires T Cell Help and Is Critical to Trained Immunity. *Cell* **175**, 1634-1650.e17 (2018).
33. Mitroulis, I. *et al.* Modulation of Myelopoiesis Progenitors Is an Integral Component of Trained Immunity. *Cell* **172**, 147-161.e12 (2018).
34. Drummer, C. *et al.* Trained Immunity and Reactivity of Macrophages and Endothelial Cells. *Arterioscler. Thromb. Vasc. Biol.* **41**, 1032–1046 (2021).
35. Teufel, L. U., Arts, R. J. W., Netea, M. G., Dinarello, C. A. & Joosten, L. A. B. IL-1 family cytokines as drivers and inhibitors of trained immunity. *Cytokine* **150**, 155773 (2022).
36. Acevedo, O. A., Berrios, R. V., Rodríguez-Guilarte, L., Lillo-Dapremont, B. & Kalergis, A. M. Molecular and Cellular Mechanisms Modulating Trained Immunity by Various Cell Types in Response to Pathogen Encounter. *Front. Immunol.* **12**, 1–11 (2021).
37. Owen, A. M., Fults, J. B., Patil, N. K., Hernandez, A. & Bohannon, J. K. TLR Agonists as Mediators of Trained Immunity: Mechanistic Insight and Immunotherapeutic Potential to Combat Infection. *Front. Immunol.* **11**, 1–25 (2021).
38. Kong, L. *et al.* Single-cell transcriptomic profiles reveal changes associated with BCG-induced trained immunity and protective effects in circulating monocytes. *Cell Rep.* **37**, 110028 (2021).
39. Moorlag, S. J. C. F. M. *et al.* An integrative genomics approach identifies KDM4 as a modulator of trained immunity. *Eur. J. Immunol.* **52**, 431–446 (2022).
40. Fanucchi, S., Domínguez-Andrés, J., Joosten, L. A. B., Netea, M. G. & Mhlanga, M. M. The Intersection of Epigenetics and Metabolism in Trained Immunity. *Immunity* **54**, 32–

- 43 (2021).
41. Arts, R. J. W. *et al.* Immunometabolic Pathways in BCG-Induced Trained Immunity. *Cell Rep.* **17**, 2562–2571 (2016).
 42. van der Meer, J. W. M., Joosten, L. A. B., Riksen, N. & Netea, M. G. Trained immunity: A smart way to enhance innate immune defence. *Mol. Immunol.* **68**, 40–4 (2015).
 43. van der Heijden, C. D. C. C. *et al.* Epigenetics and Trained Immunity. *Antioxid. Redox Signal.* **29**, 1023–1040 (2018).
 44. Saeed, S. *et al.* Epigenetic programming of monocyte-to-macrophage differentiation and trained innate immunity. *Science*. **345**, 1251086–1251086 (2014).
 45. Guilliams, M., Lambrecht, B. N. & Hammad, H. Division of labor between lung dendritic cells and macrophages in the defense against pulmonary infections. *Mucosal Immunol.* **6**, 464–73 (2013).
 46. Hussell, T. & Bell, T. J. Alveolar macrophages: Plasticity in a tissue-specific context. *Nat. Rev. Immunol.* **14**, 81–93 (2014).
 47. Guilliams, M. & Svedberg, F. R. Does tissue imprinting restrict macrophage plasticity? *Nature Immunology* vol. 22 (2021).
 48. Joshi, N., Walter, J. M. & Misharin, A. V. Alveolar Macrophages. *Cell. Immunol.* **Aug**, 86–90 (2018).
 49. Guth, A. M. *et al.* Lung environment determines unique phenotype of alveolar macrophages. *Am. J. Physiol. - Lung Cell. Mol. Physiol.* **296**, 936–946 (2009).
 50. Rubins, J. B. Alveolar macrophages: Wielding the double-edged sword of inflammation. *Am. J. Respir. Crit. Care Med.* **167**, 103–4 (2003).
 51. Aberdein, J. D., Cole, J., Bewley, M. A., Marriott, H. M. & Dockrell, D. H. Alveolar macrophages in pulmonary host defence—the unrecognized role of apoptosis as a mechanism of intracellular bacterial killing. *Clin. Exp. Immunol.* **174**, 193–202 (2013).
 52. Vernatter, J. & Pirofski, L. A. Current concepts in host-microbe interaction leading to pneumococcal pneumonia. *Curr. Opin. Infect. Dis.* **26**, 277–83 (2013).
 53. van der Poll, T. & Opal, S. M. Pathogenesis, treatment, and prevention of pneumococcal pneumonia. *Lancet* **374**, 1543–1556 (2009).
 54. Shak, J. R., Vidal, J. E. & Klugman, K. P. Influence of bacterial interactions on pneumococcal colonization of the nasopharynx. *Trends Microbiol.* **21**, 129–35 (2013).
 55. Suresh, M. V., Singh, S. K., Ferguson, D. A. & Agrawal, A. Role of the Property of C-Reactive Protein to Activate the Classical Pathway of Complement in Protecting Mice from Pneumococcal Infection. *J. Immunol.* **176**, 4369–74 (2006).
 56. Arredouani, M. *et al.* The Scavenger Receptor MARCO Is Required for Lung Defense against Pneumococcal Pneumonia and Inhaled Particles. *J. Exp. Med.* **200**, 267–272 (2004).
 57. Albiger, B. *et al.* Toll-like receptor 9 acts at an early stage in host defence against pneumococcal infection. *Cell. Microbiol.* **9**, 633–644 (2007).
 58. Bals, R. & Hiemstra, P. S. Innate immunity in the lung: How epithelial cells fight against respiratory pathogens. *Eur. Respir. J.* **23**, 327–33 (2004).
 59. Gordon, S. B., Irving, G. R. B., Lawson, R. A., Lee, M. E. & Read, R. C. Intracellular trafficking and killing of *Streptococcus pneumoniae* by human alveolar macrophages are influenced by opsonins. *Infect. Immun.* **68**, 2286–93 (2000).
 60. Dockrell, D. H. *et al.* Alveolar Macrophage Apoptosis Contributes to Pneumococcal Clearance in a Resolving Model of Pulmonary Infection. *J. Immunol.* **171**, 5380–8 (2003).

61. Sato, S. *et al.* Role of Galectin-3 as an Adhesion Molecule for Neutrophil Extravasation During Streptococcal Pneumonia. *J. Immunol.* **168**, 1813–22 (2002).
62. Hare, K. M., Morris, P., Smith-Vaughan, H. & Leach, A. J. Random colony selection versus colony morphology for detection of multiple pneumococcal serotypes in nasopharyngeal swabs. *Pediatr. Infect. Dis. J.* **27**, 178–80 (2008).
63. Rijneveld, A. W., de Vos, A. F., Florquin, S., Verbeek, J. S. & van der Poll, T. CD11b Limits Bacterial Outgrowth and Dissemination during Murine Pneumococcal Pneumonia. *J. Infect. Dis.* **191**, 1755–60 (2005).
64. Gomez Perdiguero, E. *et al.* Tissue-resident macrophages originate from yolk-sac-derived erythro-myeloid progenitors. *Nature* **518**, 547–51 (2015).
65. Hoeffel, G. *et al.* C-Myb⁺ Erythro-Myeloid Progenitor-Derived Fetal Monocytes Give Rise to Adult Tissue-Resident Macrophages. *Immunity* **42**, 665–78 (2015).
66. Guilliams, M. *et al.* Alveolar macrophages develop from fetal monocytes that differentiate into long-lived cells in the first week of life via GM-CSF. *J. Exp. Med.* **210**, 1977–92 (2013).
67. Machiels, B. *et al.* A gammaherpesvirus provides protection against allergic asthma by inducing the replacement of resident alveolar macrophages with regulatory monocytes. *Nat. Immunol.* **18**, 1310–1320 (2017).
68. Hashimoto, D. *et al.* Tissue-resident macrophages self-maintain locally throughout adult life with minimal contribution from circulating monocytes. *Immunity* **38**, 792–804 (2013).
69. Machiels, B. *et al.* A gammaherpesvirus provides protection against allergic asthma by inducing the replacement of resident alveolar macrophages with regulatory monocytes. *Nat. Immunol.* **18**, 1310–1320 (2017).
70. Camilli, G., Tabouret, G. & Quintin, J. The Complexity of Fungal β -Glucan in Health and Disease: Effects on the Mononuclear Phagocyte System. *Front. Immunol.* **16**, (2018).
71. Han, B., Baruah, K., Cox, E., Vanrompay, D. & Bossier, P. Structure-Functional Activity Relationship of β -Glucans From the Perspective of Immunomodulation: A Mini-Review. *Front. Immunol.* **11**, (2020).
72. Rice, P. J. *et al.* Pharmacokinetics of fungal (1-3)- β -D-glucans following intravenous administration in rats. *Int. Immunopharmacol.* **4**, 1209–1215 (2004).
73. Williams, D. L. *et al.* Pre-clinical safety evaluation of soluble glucan. *Int. J. Immunopharmacol.* **10**, 405–414 (1988).
74. Svozil, V., Král, V., Dobiášová, L. R., Stiborová, I. & Vetvicka, V. Clinical trials of yeast-derived β -(1,3) glucan in children: Effects on innate immunity. *Ann. Transl. Med.* **2**, 1–6 (2014).
75. Graubaum, H.-J., Busch, R., Stier, H. & Gruenwald, J. A Double-Blind, Randomized, Placebo-Controlled Nutritional Study Using an Insoluble Yeast Beta-Glucan to Improve the Immune Defense System. *Food Nutr. Sci.* **03**, 738–746 (2012).
76. Geller, A., Shrestha, R. & Yan, J. Yeast-derived β -glucan in cancer: Novel uses of a traditional therapeutic. *Int. J. Mol. Sci.* **20**, 1–20 (2019).
77. Jin, Y., Li, P. & Wang, F. β -glucans as potential immunoadjuvants: A review on the adjuvanticity, structure-activity relationship and receptor recognition properties. *Vaccine* **36**, 5235–5244 (2018).
78. Roudi, R., Mohammadi, S. R., Roudbary, M. & Mohsenzadegan, M. Lung cancer and β -glucans: review of potential therapeutic applications. *Invest. New Drugs* **35**, 509–517 (2017).

79. Bashir, K. M. I. & Choi, J. S. Clinical and physiological perspectives of β -glucans: The past, present, and future. *International Journal of Molecular Sciences* vol. 18 (2017).
80. Kleinnijenhuis, J. *et al.* Long-lasting effects of bcg vaccination on both heterologous th1/th17 responses and innate trained immunity. *J. Innate Immun.* **6**, 152–158 (2014).
81. Kleinnijenhuis, J. *et al.* Bacille Calmette-Guérin induces NOD2-dependent nonspecific protection from reinfection via epigenetic reprogramming of monocytes. *Proc. Natl. Acad. Sci. U. S. A.* **109**, 17537–17542 (2012).
82. Netea, M. G. *et al.* Trained immunity: A program of innate immune memory in health and disease. *Science.* **352**, (2016).
83. Li, X. *et al.* Maladaptive innate immune training of myelopoiesis links inflammatory comorbidities. *Cell* **185**, 1709-1727.e18 (2022).
84. Bekkering, S. *et al.* Oxidized low-density lipoprotein induces long-term proinflammatory cytokine production and foam cell formation via epigenetic reprogramming of monocytes. *Arterioscler. Thromb. Vasc. Biol.* **34**, 1731–1738 (2014).
85. Zhong, C., Yang, X., Feng, Y. & Yu, J. Trained Immunity: An Underlying Driver of Inflammatory Atherosclerosis. *Front. Immunol.* **11**, (2020).
86. Damjanovic, D., Lai, R., Jeyanathan, M., Hogaboam, C. M. & Xing, Z. Marked improvement of severe lung immunopathology by influenza-associated pneumococcal superinfection requires the control of both bacterial replication and host immune responses. *Am. J. Pathol.* **183**, 868–880 (2013).
87. Neupane, A. S. *et al.* Patrolling Alveolar Macrophages Conceal Bacteria from the Immune System to Maintain Homeostasis. *Cell* **183**, (2020).
88. Lanz-Mendoza, H. & Contreras-Garduño, J. Innate immune memory in invertebrates: Concept and potential mechanisms. *Dev. Comp. Immunol.* **127**, (2022).
89. Reimer-Michalski, E. M. & Conrath, U. Innate immune memory in plants. *Semin. Immunol.* **28**, 319–327 (2016).
90. Netea, M. G. *et al.* Trained Immunity: a Tool for Reducing Susceptibility to and the Severity of SARS-CoV-2 Infection. *Cell* **181**, 969–977 (2020).
91. Arafa, E. I. *et al.* Recruitment and training of alveolar macrophages after pneumococcal pneumonia. *JCI Insight* **7**, e150239 (2022).
92. Demir, G., Klein, H. O., Mandel-Molinas, N. & Tuzuner, N. Beta glucan induces proliferation and activation of monocytes in peripheral blood of patients with advanced breast cancer. *Int. Immunopharmacol.* **7**, 113–6 (2007).
93. Pechous, R. D. With friends like these: The complex role of neutrophils in the progression of severe pneumonia. *Front. Cell. Infect. Microbiol.* **7**, (2017).

6.0 – Figures

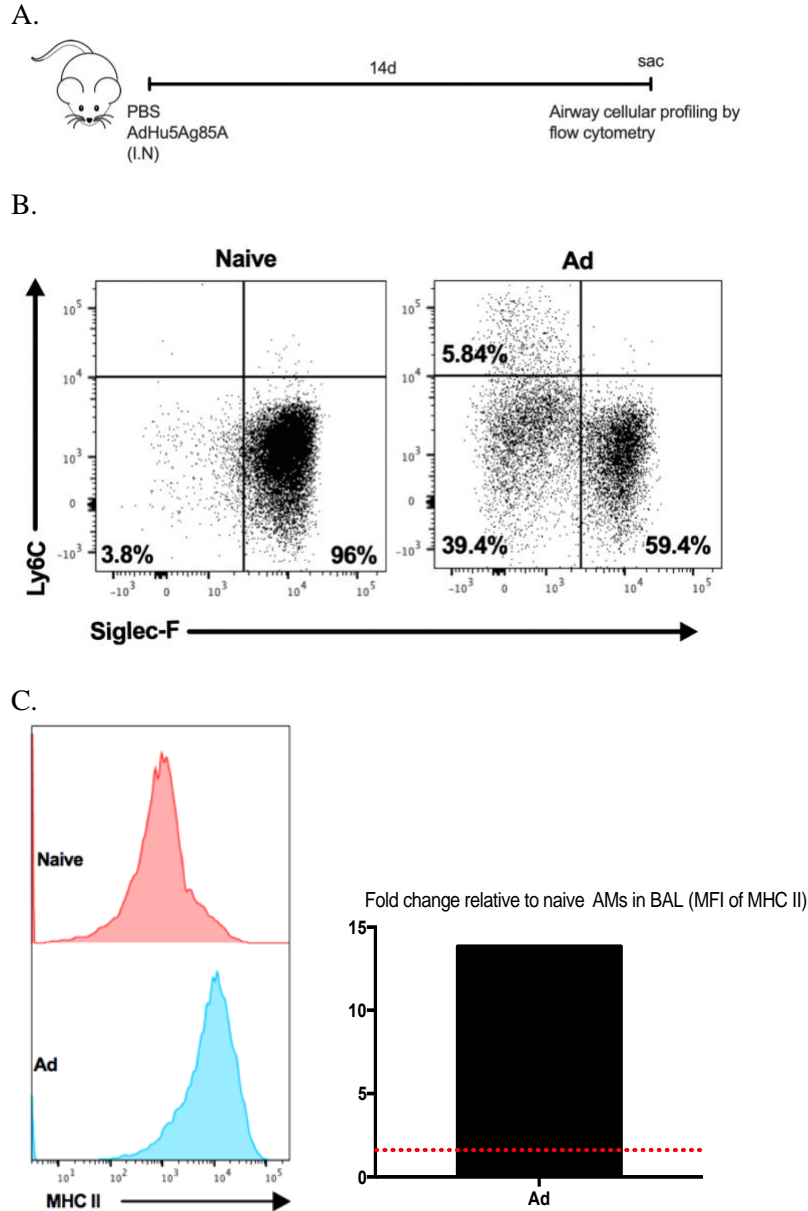


Figure 1: Respiratory mucosal delivery of an Ad-vectored vaccine generated memory AMs with upregulated MHC II expression. A) Schema. B) Dot plots showing the different cell populations in BAL for each treatment group (Alveolar Macrophage - Q3, Interstitial Macrophage - Q4 and Monocyte Derived Macrophages - Q1). C) Offset histograms showing MHC II expression in AMs of BAL between naïve and Ad group and a bar graph with the fold change relative to naïve AMs in BAL (MFI of MHC II). Data in B & C are representative of one individual experiment (n=1 mouse/group).

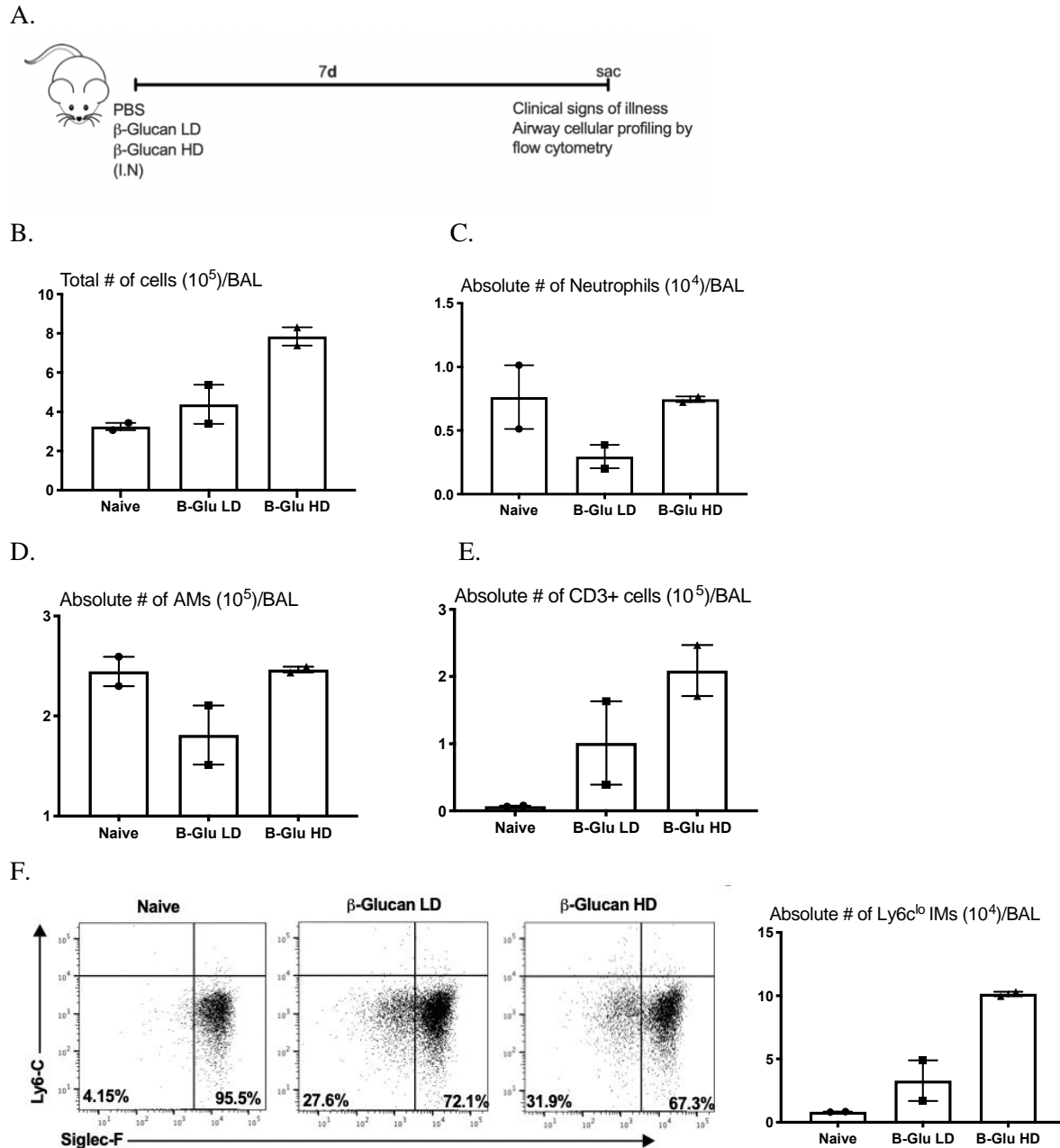
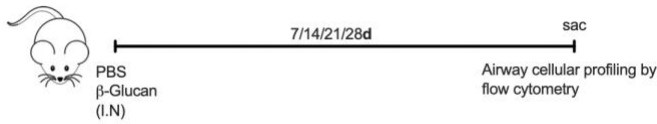
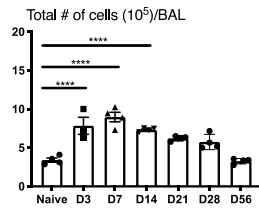


Figure 2: Inflammatory cellular responses in the airways at 7 days following intranasal delivery of a low dose (LD) or high dose (HD) of β -Glucan. A) Schema. B) Total cell counts for BAL. C) Absolute cell numbers of Neutrophils in the BAL. D) Absolute cell numbers of AMs in the BAL. E) Absolute numbers of CD3+ T Cells in the BAL. F) Dot plots of the terminal gate of the gating strategy with Siglec-F and Ly6C showing the different cell populations in the BAL for each treatment group (Alveolar Macrophage - Q3, Interstitial Macrophage - Q4 and Monocyte Derived Macrophages - Q1) and absolute cell numbers of IMs. All bar graphs are presented as mean \pm SEM. Data in B-F are representative of one individual experiment (n=2 mice/group).

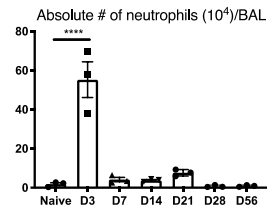
A.



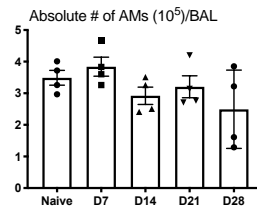
B.



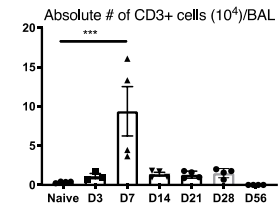
C.



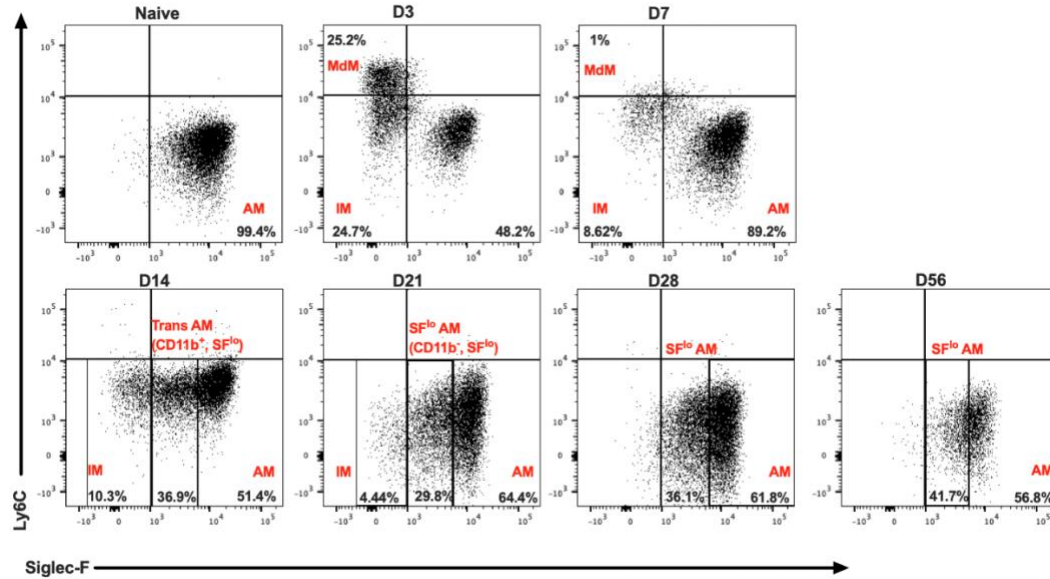
D.



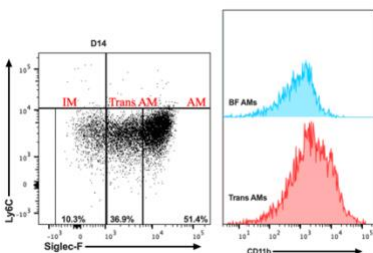
E.



F.



G.



H.

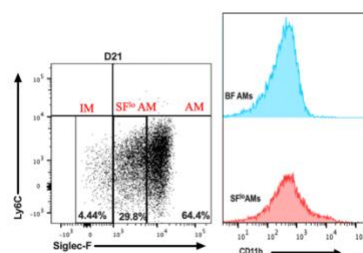
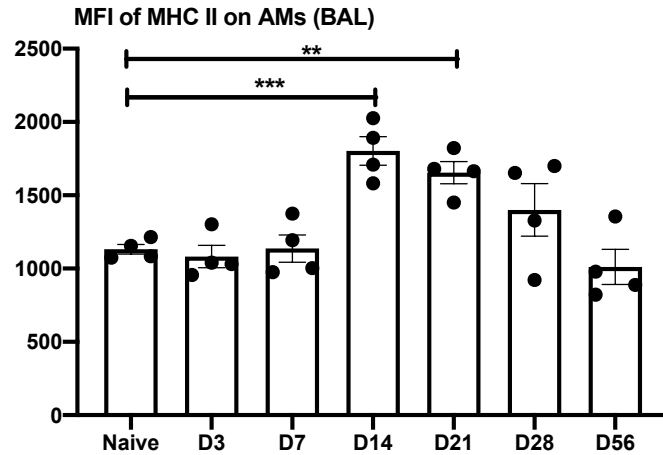


Figure 3: Significant and persistent alterations in the airway cellular profile and macrophage phenotype at various timepoints post-intranasal delivery of β -Glucan. A) Schema. B) Total cell counts (BAL). C-E) Absolute cell numbers of neutrophils, AMs and CD3+ cells (BAL). F) Dot plots of terminal gate of with Siglec-F and Ly6C showing the different cell populations (Alveolar Macrophage - Q3, Interstitial Macrophage - Q4 and Monocyte Derived Macrophages - Q1) at d3, 7, 14, 21, 28 and 56. G and H) terminal dot plots at d14 and d28 with different macrophage populations labelled accordingly and offset histograms comparing expression of CD11b. Data in B-H are representative of one individual experiment (n=4)

mice/group). All bar graphs are presented as mean \pm SEM. Statistical analyses for B,C and E were ordinary one-way ANOVAs with multiple comparisons. * $p < 0.05$, ** $p < 0.01$, *** $p < 0.001$, **** $p < 0.0001$.

A.



B.

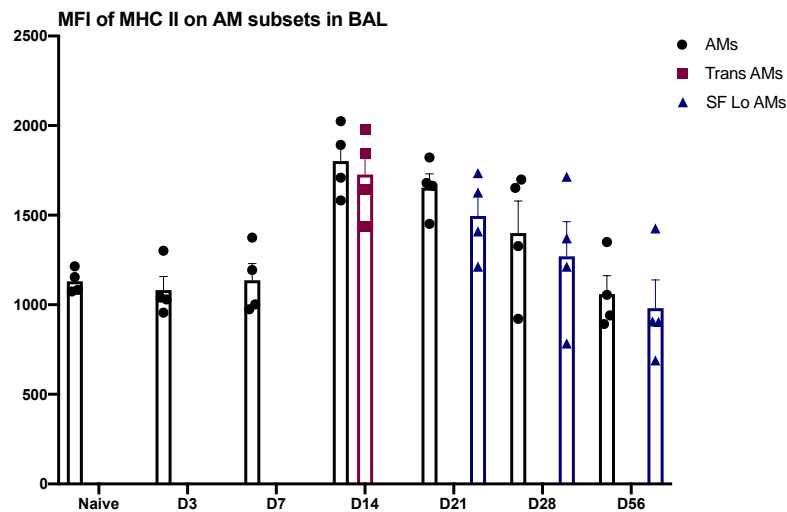


Figure 4: Time-dependent upregulation of MHC II expression in airway macrophages following intranasal delivery of β -Glucan. A) Bar graph showing MFI of MHC II on AMs following i.n delivery of β -Glucan. B) Bar graph showing MFI of MHC II on different airway macrophage subsets following i.n delivery of β -Glucan. All bar graphs are presented as mean \pm SEM. Data in A and B are representative of one independent experiment (n=4 mice/group). Statistical analyses for A were performed using 2-way ANOVAs with multiple comparisons. * $p < 0.05$, ** $p < 0.01$, *** $p < 0.001$, **** $p < 0.0001$.

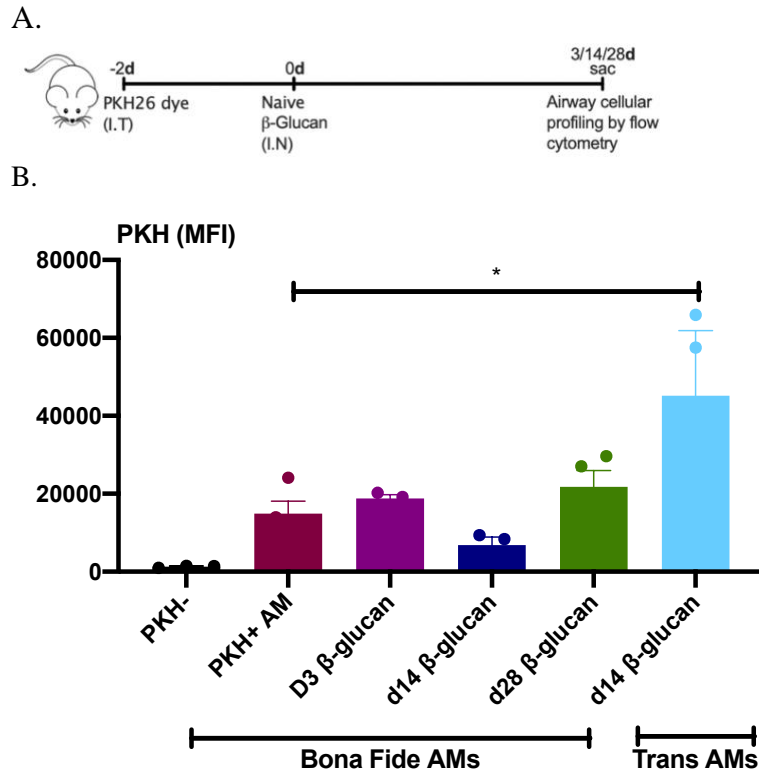


Figure 5: Significant recruitment and differentiation of circulating monocytes to bona fide AMs following intranasal delivery of β -Glucan. A) Schema. B) Measure of MFI of PKH signal on bona fide AMs (Siglec-F⁺Ly6c-CD11b⁻) and on Trans AMs (Siglec-F^{lo}Ly6c-CD11b⁺). All bar graphs are presented as mean \pm SEM. Data in B is representative of one independent experiment (n=4 mice/group). Statistical analyses for A were performed using a one-way ANOVA. * p < 0.05, ** p < 0.01, *** p < 0.001, **** p < 0.0001.

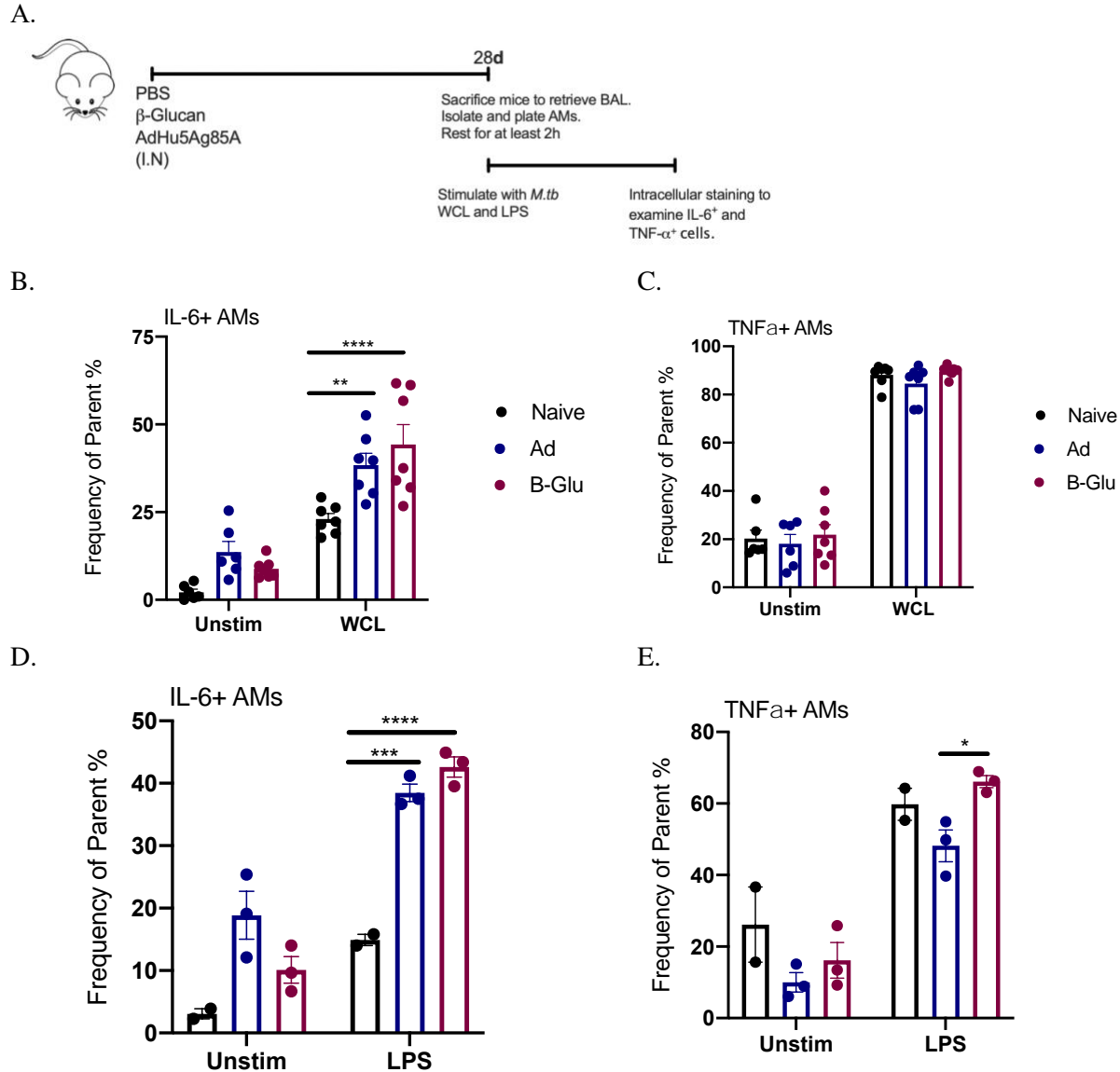


Figure 6: Cytokine production by Ad vaccine- or β -Glucan-trained airway macrophages in response to ex vivo re-stimulation with inflammatory agents (WCL or LPS). A) Schema. B) Bar graph showing frequency of parent (%) of AMs that are IL-6+ in various groups with or without stimulation with WCL. C) Bar graph showing frequency of parent (%) of AMs that are TNF- α + in various groups with or without WCL stimulation. D) Bar graph showing frequency of parent (%) of AMs that are IL-6+ in various groups with or without LPS stimulation. E) Bar graph showing frequency of parent (%) of AMs that are TNF- α + in various groups with or without LPS stimulation. All bar graphs are presented as mean \pm SEM. Data in B and C is representative of two individual experiments (n=7 mice/group for WCL stimulation, n=3 mice/group for LPS stimulation). Statistical analyses for Data in B-E were performed using 2-way ANOVAs with multiple comparisons. * $p < 0.05$, ** $p < 0.01$, *** $p < 0.001$, **** $p < 0.0001$.

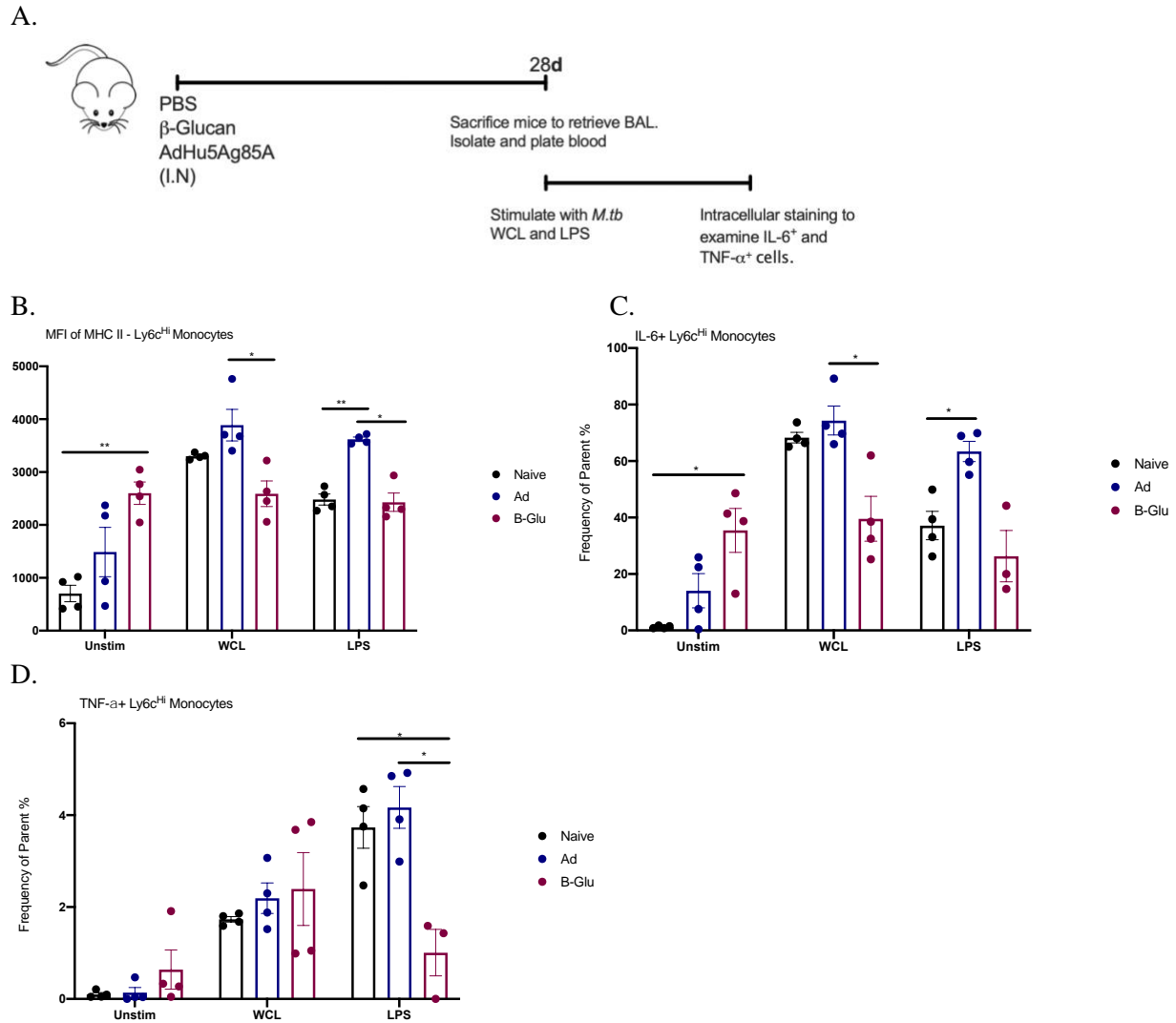
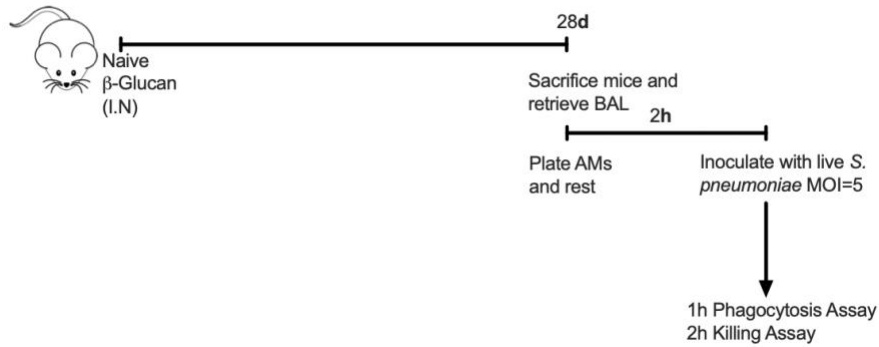
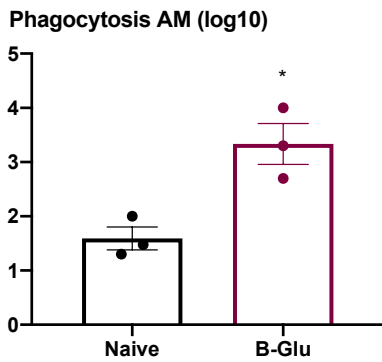


Figure 7: Changes in circulating monocytes following intranasal delivery of β -Glucan. A) Schema. B) Bar graphs showing MFI of MHC II on Ly6C^{hi} monocytes in various groups with WCL/LPS/no stimulation C) Bar graphs showing frequency of parent (%) of Ly6C^{hi} monocytes that are IL-6+ in various groups with WCL/LPS/no stimulation. D) Bar graphs showing frequency of parent (%) of Ly6C^{hi} monocytes that are TNF- α + in various groups with WCL/LPS/no stimulation. All bar graphs are presented as mean \pm SEM. Data in B-D is representative of one individual experiment (n=4 mice/group). Statistical analyses for Data in B-D were performed using 2-way ANOVAs with multiple comparisons. * p < 0.05, ** p < 0.01, *** p < 0.001, **** p < 0.0001.

A.



B.



C.

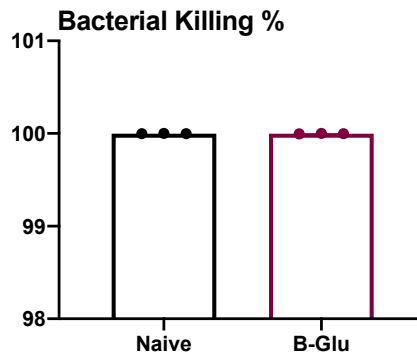
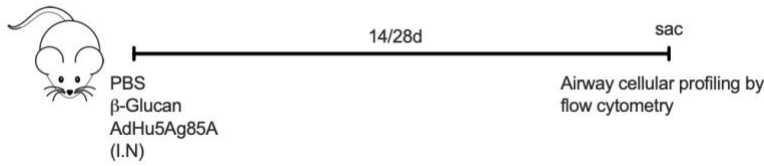
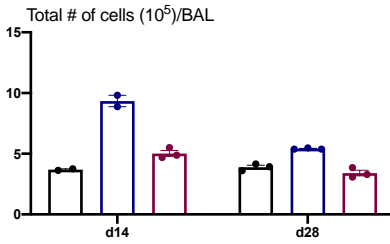


Figure 8: Assessment of bacterial phagocytosis and killing by β-Glucan-trained airway macrophages. A) Schema. B) Bar graph depicting log₁₀ bacterial CFU phagocytosed as part of the phagocytosis assay. C) Bar graph depicting % of bacterial killing. Bar graphs are presented as mean ± SEM. Data is representative of one individual experiment (n=3 mice/group). Statistical analysis for data in B was performed using a two-tailed t-test. * p < 0.05, ** p < 0.01, *** p < 0.001, **** p < 0.0001.

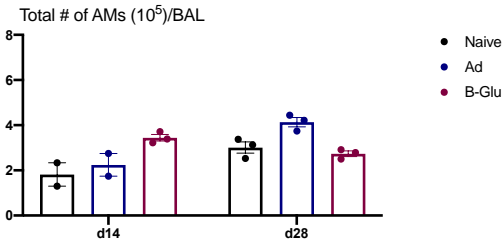
A.



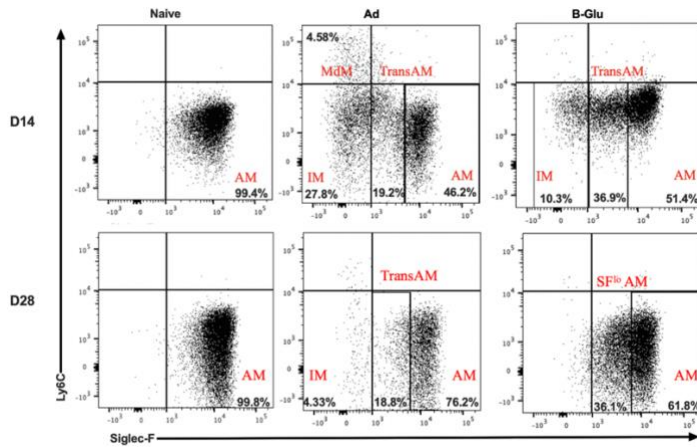
B.



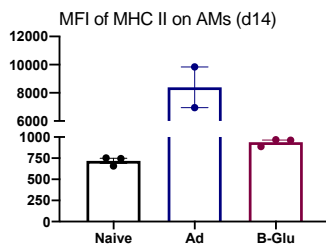
C.



D.



E.



F.

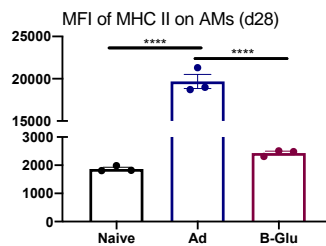


Figure 9: Differential airway cellular responses to intranasal delivery of β-Glucan and Ad-vectored vaccine. A) Schema. B and C) Bar graphs showing total number of cells in the BAL and absolute numbers of AMs in the same. D) Dot plots of the terminal gate of the gating strategy with Siglec-F and Ly6C showing the different cell populations in the BAL for each treatment group (Alveolar Macrophage - Q3, Interstitial Macrophage - Q4 and Monocyte Derived Macrophages - Q1) at d14 and 28. E and F) Bar graphs showing MFI of MHC II on AMs in different treatment groups at d14 and 28. All bar graphs are presented as mean ± SEM. Data in B-F are representative of one individual experiment (n=3 mice/group). Statistical

analyses for Data in E and F were performed using 2-way ANOVAs with multiple comparisons. * $p < 0.05$, ** $p < 0.01$, *** $p < 0.001$, **** $p < 0.0001$.

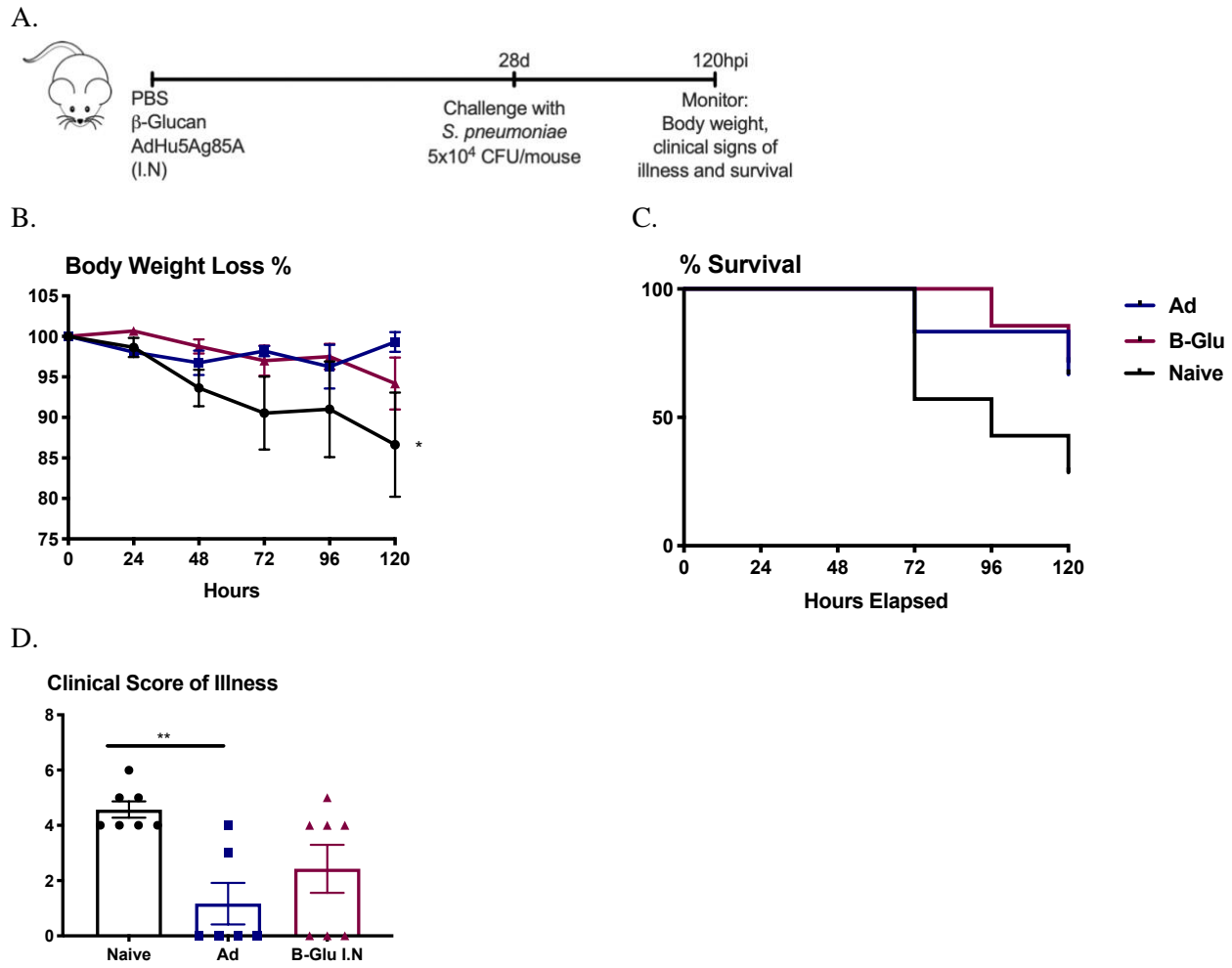


Figure 10: TII elicited by intranasal delivery of β -Glucan or Ad-vectored vaccine provides enhanced protection against clinical outcomes from heterologous *S. pneumoniae* infection. A) Schema. B) Percentage of body weight loss following bacterial infection. C) % Survival graph of mice, following a lethal dose of *S. pneumoniae*. D) Clinical score of illness following bacterial infection. All bar graphs are presented as mean \pm SEM. Data in B-D are representative of one individual experiment ($n=7$ mice/group except Ad where $n=6$ mice). Statistical analysis for B was performed using Survival curve comparisons. Statistical analysis for D was performed using an ordinary one-way ANOVA with multiple comparisons. * $p < 0.05$, ** $p < 0.01$, *** $p < 0.001$, **** $p < 0.0001$.

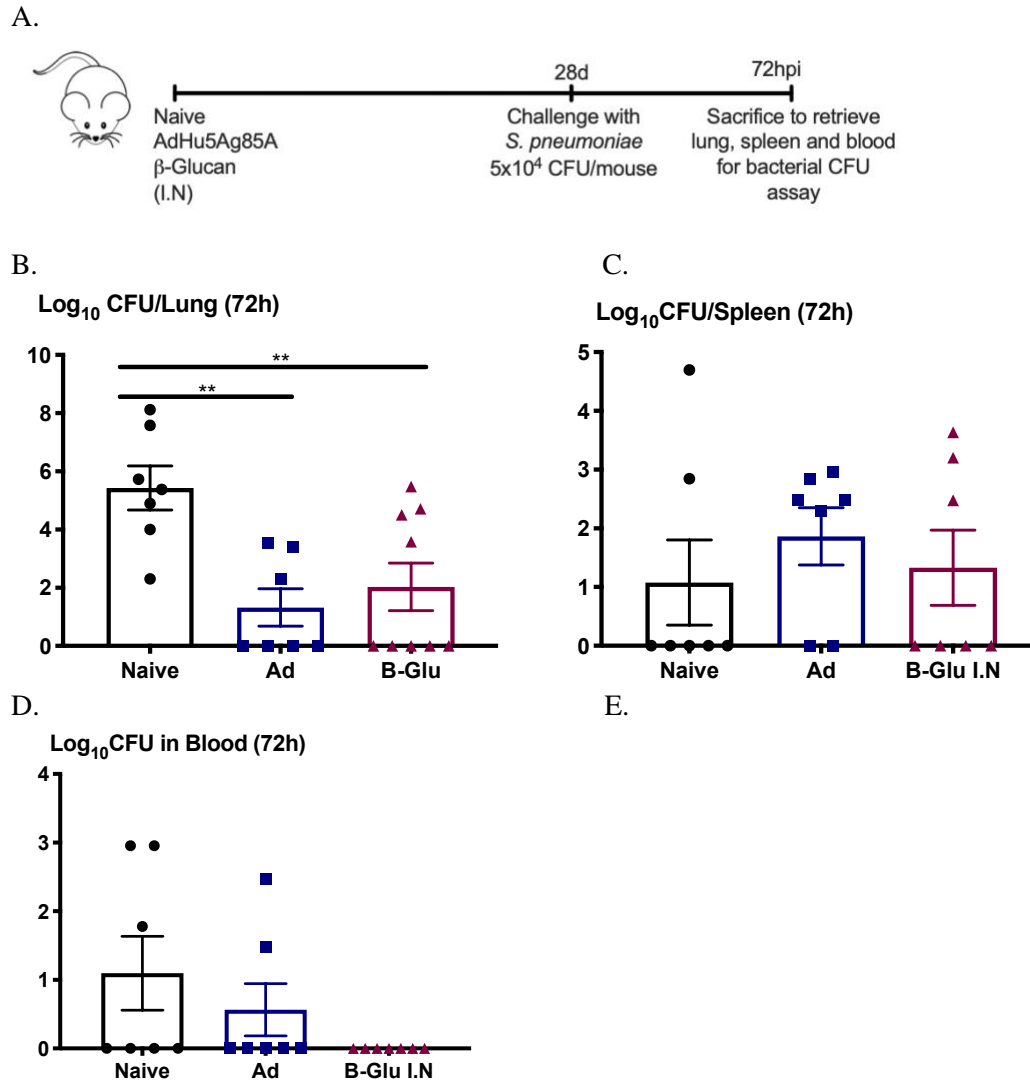


Figure 11: TII elicited by intranasal delivery of β -Glucan or Ad-vectored vaccine provides enhanced control of *S. pneumoniae* infection in the lung. A) Schema. B) Bacterial CFU in the lung at 72h post-infection. C and D) Bacterial CFU in the spleen and blood, respectively, at 72h post-infection. Bar graphs are presented as mean \pm SEM. Data in B-D are representative of two independent experiments (n= 4 (1st experiment) mice/group and n=5 (2nd experiment) mice/group). Statistical analysis for B was performed using an ordinary one-way ANOVA with multiple comparisons. * p < 0.05, ** p < 0.01, *** p < 0.001, **** p < 0.0001.

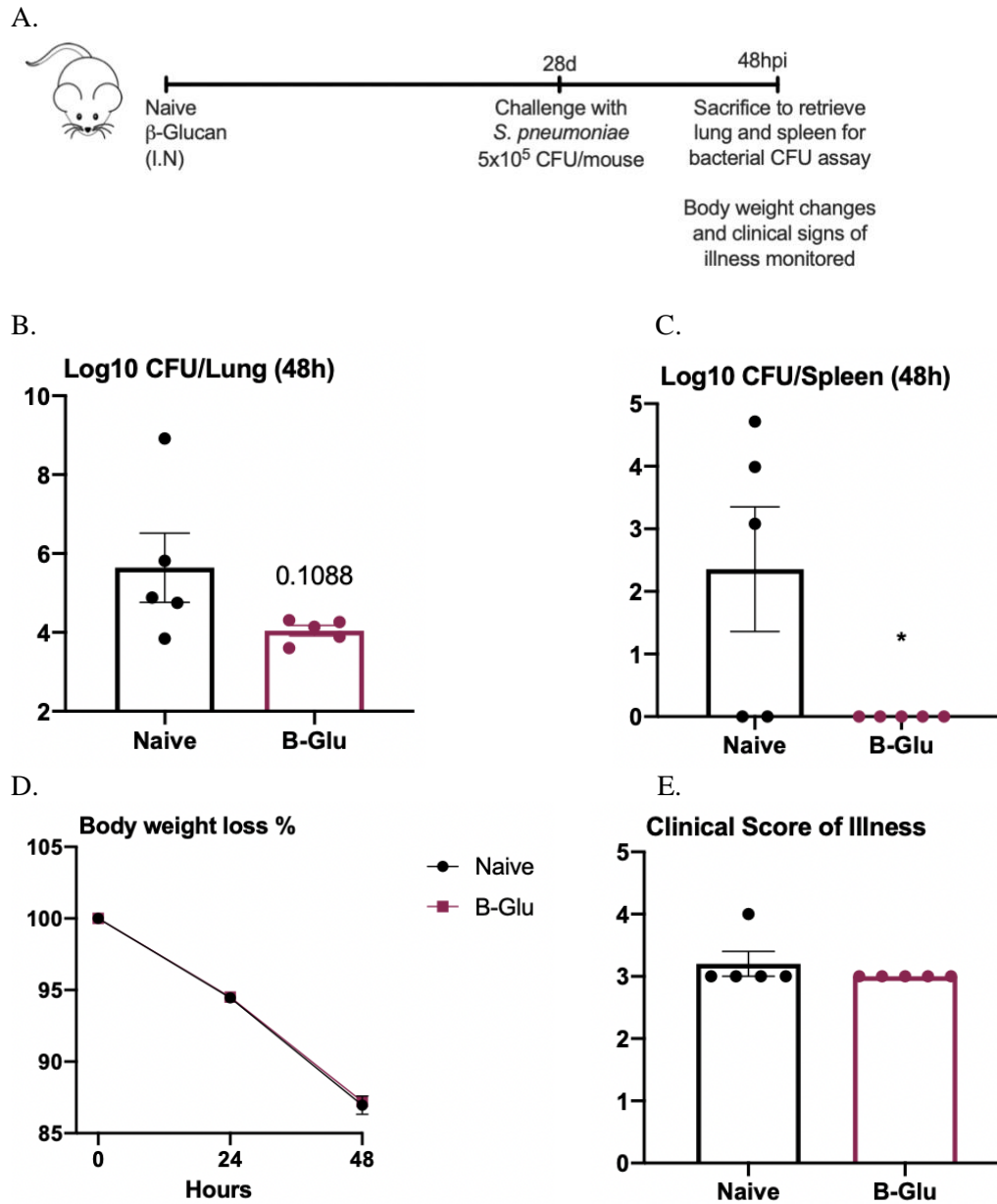
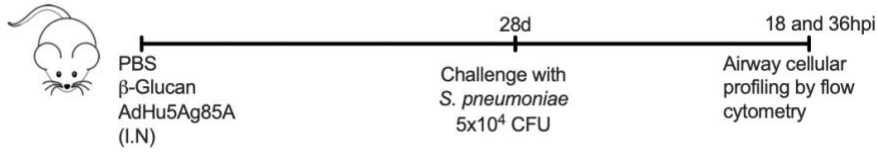
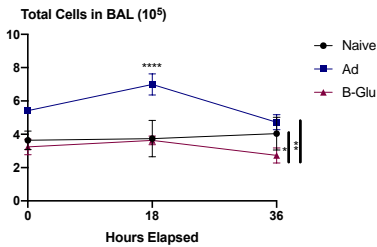


Figure 12: Repeat assessment of intranasal β-Glucan exposure-mediated protection against heterologous bacterial infection. A) Schema. (B) Bacterial CFU in the lung at 48h post-infection. (C) Bacterial CFU in the spleen at 48h post-infection. (D) Percentage of body weight loss following bacterial infection. (D) Clinical scores of illness following bacterial infection. All bar graphs are presented as mean ± SEM. Data in B-E are representative of one independent experiment (n=5 mice/group). Statistical analyses of data in B and C were performed using unpaired t-tests. * p < 0.05, ** p < 0.01, *** p < 0.001, **** p < 0.0001.

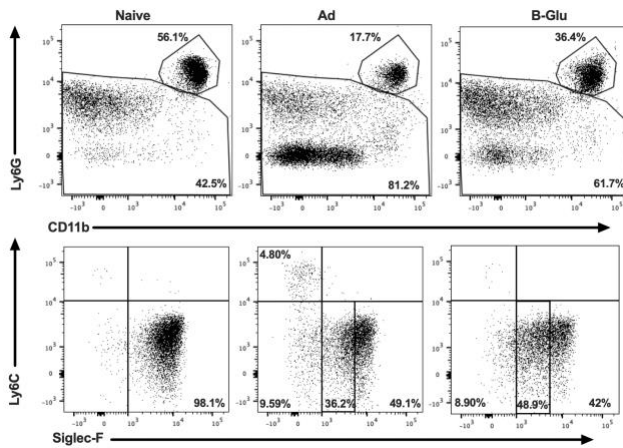
A.



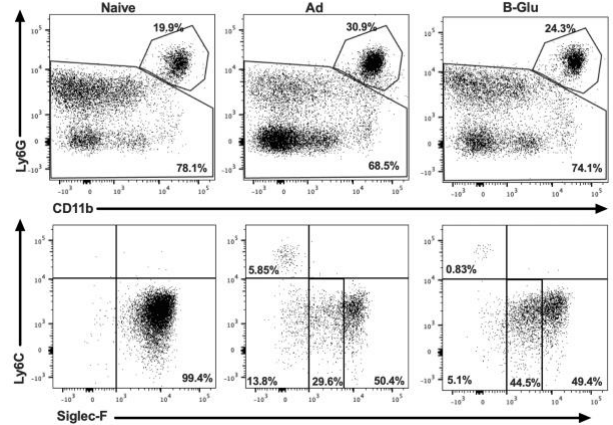
B.



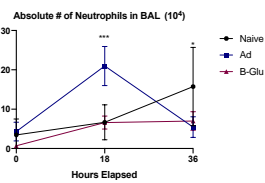
C.



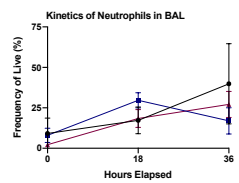
D.



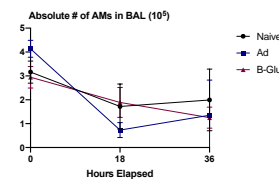
E.



F.



G.



H.

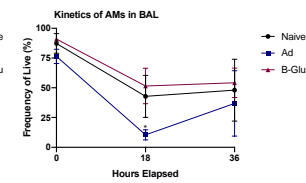
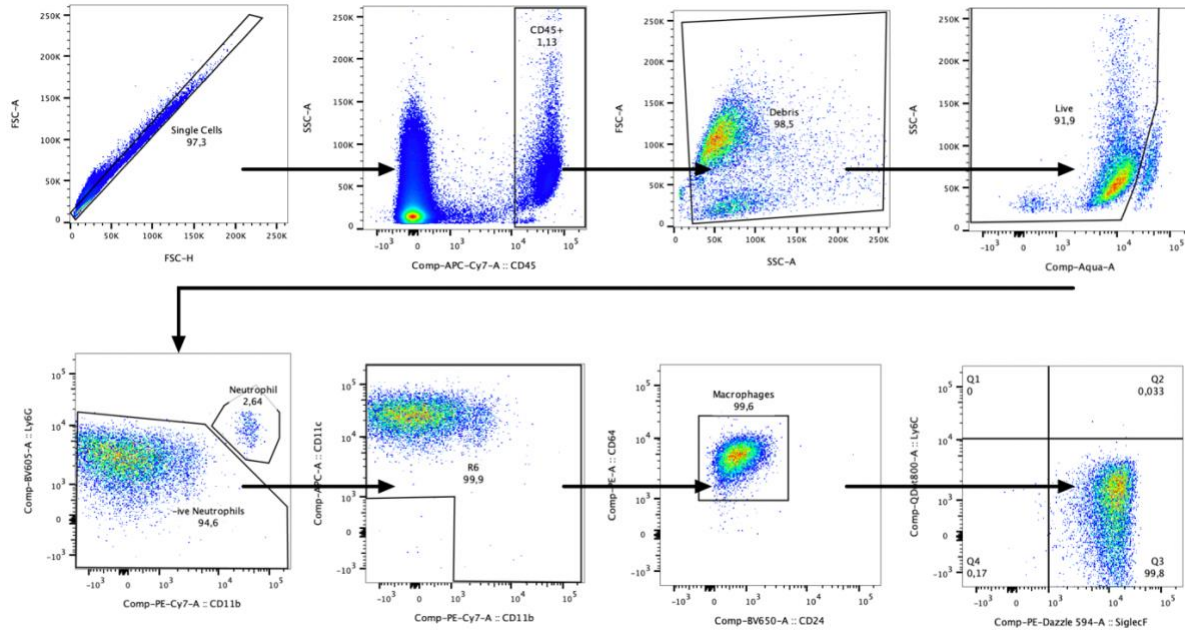


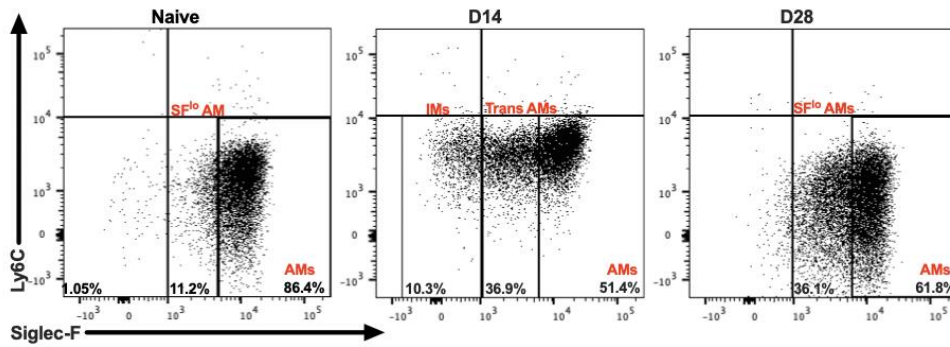
Figure 13: Differential airway immune responses to *S. pneumoniae* infection following intranasal delivery of β -Glucan and Ad-vectored vaccine. A) Schema. B) Line graph showing total number of cells in the BAL. C and D) Dot plots of the neutrophil and terminal gate (supplementary figure 1) at **18 (C)** and **36 h (D)** post-infection. E-H) Line graphs showing absolute number and frequency of live of neutrophils and AMs in different treatment groups at 18 and 36h post-infection. All line graphs are presented as mean \pm SEM. Data in B-H are representative of one independent experiment (n=4 mice/group).

Statistical analyses in B, E-H were performed using 2-way ANOVAs with multiple comparisons. * $p < 0.05$, ** $p < 0.01$, *** $p < 0.001$, **** $p < 0.0001$.

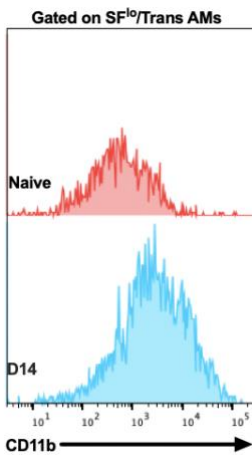


Supplementary Figure 1: Gating strategy for identification of pulmonary macrophage populations

A.



B.



Supplementary Figure 2: Naïve airways have a small population of SF^{lo} AMs that is differential to populations seen following intranasal delivery of β-Glucan. A) Dot plots of the terminal gate of the gating strategy with Siglec-F and Ly6C showing the different cell populations in the BAL for each treatment group (Alveolar Macrophage - Q3, Interstitial Macrophage - Q4 and Monocyte Derived Macrophages - Q1) at d0,14 and 28. B) Offset histogram showing CD11b expression in SF^{lo} AMs (naïve) and Trans AMs (day 14 post-β-Glucan exposure) of BAL. Data for A and B was taken from the experiment performed in Figure 3, representative of one individual experiment (n=4 mice/group).

